



HAL
open science

Distribution and (palaeo)ecological affinities of the main Spiniferites taxa in the mid-high latitudes of the Northern Hemisphere

Anne de Vernal, Frederique Eynaud, Maryse Henry, Audrey Limoges, Laurent Londeix, Jens Matthiessen, Fabienne Marret, Vera Pospelova, Taoufik Radi, André Rochon, et al.

► To cite this version:

Anne de Vernal, Frederique Eynaud, Maryse Henry, Audrey Limoges, Laurent Londeix, et al.. Distribution and (palaeo)ecological affinities of the main Spiniferites taxa in the mid-high latitudes of the Northern Hemisphere. *Palynology*, 2018, 42 (sup1), pp.182-202. 10.1080/01916122.2018.1465730 . hal-04557857

HAL Id: hal-04557857

<https://hal.science/hal-04557857>

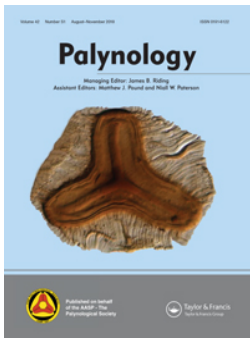
Submitted on 24 Apr 2024

HAL is a multi-disciplinary open access archive for the deposit and dissemination of scientific research documents, whether they are published or not. The documents may come from teaching and research institutions in France or abroad, or from public or private research centers.

L'archive ouverte pluridisciplinaire **HAL**, est destinée au dépôt et à la diffusion de documents scientifiques de niveau recherche, publiés ou non, émanant des établissements d'enseignement et de recherche français ou étrangers, des laboratoires publics ou privés.



Distributed under a Creative Commons Attribution - NonCommercial - NoDerivatives 4.0 International License



Distribution and (palaeo)ecological affinities of the main *Spiniferites* taxa in the mid-high latitudes of the Northern Hemisphere

Anne de Vernal, Frédérique Eynaud, Maryse Henry, Audrey Limoges, Laurent Londeix, Jens Matthiessen, Fabienne Marret, Vera Pospelova, Taoufik Radi, André Rochon, Nicolas Van Nieuwenhove & Sébastien Zaragosi

To cite this article: Anne de Vernal, Frédérique Eynaud, Maryse Henry, Audrey Limoges, Laurent Londeix, Jens Matthiessen, Fabienne Marret, Vera Pospelova, Taoufik Radi, André Rochon, Nicolas Van Nieuwenhove & Sébastien Zaragosi (2018) Distribution and (palaeo)ecological affinities of the main *Spiniferites* taxa in the mid-high latitudes of the Northern Hemisphere, *Palynology*, 42:sup1, 182-202, DOI: [10.1080/01916122.2018.1465730](https://doi.org/10.1080/01916122.2018.1465730)

To link to this article: <https://doi.org/10.1080/01916122.2018.1465730>



© 2018 The Author(s). Published by AASP – The Palynological Society.



Published online: 14 Dec 2018.



Submit your article to this journal [↗](#)



Article views: 1530



View related articles [↗](#)



View Crossmark data [↗](#)



Citing articles: 6 View citing articles [↗](#)



Distribution and (palaeo)ecological affinities of the main *Spiniferites* taxa in the mid-high latitudes of the Northern Hemisphere

Anne de Vernal^a, Frédérique Eynaud^b, Maryse Henry^a, Audrey Limoges^{c*}, Laurent Londeix^b, Jens Matthiessen^d, Fabienne Marret^e, Vera Pospelova^f, Taoufik Radi^a, André Rochon^g, Nicolas Van Nieuwenhove^{c,h*} and Sébastien Zaragosi^b

^aGeotop Université du Québec à Montréal, Montréal, Canada; ^bUniversité de Bordeaux, UMR 5805 EPOC, Pessac cedex, France; ^cGeological Survey of Denmark and Greenland (GEUS), Copenhagen, Denmark; ^dAlfred Wegener Institute, Bremerhaven, Germany; ^eSchool of Environmental Sciences, University of Liverpool, Liverpool, UK; ^fSchool of Earth and Ocean Sciences, University of Victoria, Victoria, Canada; ^gInstitut des sciences de la mer de Rimouski (ISMER), Université du Québec à Rimouski, Rimouski, Canada; ^hDepartment of Geoscience, Aarhus University, Aarhus, Denmark

ABSTRACT

In marine sediments of late Cenozoic age, *Spiniferites* is a very common genus of dinoflagellate cysts (dinocysts). Despite some taxonomical ambiguities due to large range of morphological variations within given species and convergent morphologies between different species, the establishment of an operational taxonomy permitted to develop a standardized modern database of dinocysts for the mid-high latitudes of the Northern Hemisphere. In the database that includes 1490 surface sediment samples, *Spiniferites mirabilis-hyperacanthus*, *Spiniferites ramosus* and *Spiniferites elongatus* were counted in addition to *Spiniferites belerius*, *Spiniferites bentorii*, *Spiniferites bulloideus*, *Spiniferites delicatus*, *Spiniferites lazus* and *Spiniferites membranaceus*. Among these taxa, *Spiniferites mirabilis-hyperacanthus*, *Spiniferites ramosus*, and *Spiniferites elongatus* are easy to identify and are particularly common. *Spiniferites bentorii* and *Spiniferites delicatus* also are morphologically distinct and occur in relatively high percentages in many samples. *Spiniferites lazus* and *Spiniferites membranaceus* also bear distinctive features, but occur only in a few samples. The identification of other taxa (*Spiniferites belerius*, *Spiniferites bulloideus*, notably) may be equivocal and their reported distribution has to be used with caution. The spatial distribution of *Spiniferites* species, with emphasis on the five most common taxa, is documented here with reference to hydrography (salinity and temperature in winter and summer, sea ice cover), primary productivity and geographical setting (bathymetry, distance to the coastline). The results demonstrate distinct ecological affinities for *Spiniferites elongatus*, which has an Arctic-subarctic distribution and appears abundant in low productivity environments characterized by winter sea ice and large temperature contrast between winter and summer. *Spiniferites mirabilis-hyperacanthus*, which occurs in warm temperate water sites, is more abundant in high salinity environments. It shares its environmental domain with *Spiniferites bentorii*, which appears to have a narrower distribution towards the warm and high salinity end of the *Spiniferites mirabilis-hyperacanthus* distribution. In contrast, *Spiniferites delicatus*, which occurs in warm-temperate to tropical environments, shows preference for relatively low salinity and low seasonal contrasts of temperature. *Spiniferites ramosus* exhibits a particularly wide distribution that overlaps both cold and warm *Spiniferites* taxa. Its cosmopolitan occurrence and its long-ranging biostratigraphical distribution suggest a high plasticity of the species and/or co-occurrence of several cryptic species. Hence, whereas *Spiniferites elongatus* and *Spiniferites mirabilis-hyperacanthus* are useful palaeoecological indicators despite their large morphological variability, *Spiniferites ramosus* is a taxon with an unconstrained ecological significance.

KEYWORDS

Dinocysts; Quaternary; palaeoceanography; temperature; salinity; sea-ice; productivity

1. Introduction

Spiniferites Mantell 1850 is a very common dinoflagellate cyst (dinocyst) genus in Mesozoic and Cenozoic sediments of the world oceans. More than one hundred species have been formally described and more than twenty of them were reported from Quaternary deposits (Williams et al. 2017; Londeix et al. 2018; Mertens et al. 2018). However, whereas *Spiniferites* is one of the most common genera of recent and

past dinocyst populations, its use in palaeoecology and palaeoclimatology is not straightforward due to difficulties encountered for identification to species level. These difficulties arise from large morphological variations that characterize many species and/or morphological convergence between different species. Hence, the assignment of *Spiniferites* taxa to a given species from routine observation in optical microscopy is sometimes subjective and many

CONTACT Anne de Vernal devernal.anne@uqam.ca

*Present address: Department of Earth Sciences, University of New Brunswick, 2 Bailey Drive, Fredericton, NB E3B 5A3, Canada.

© 2018 The Author(s). Published by AASP – The Palynological Society.

This is an Open Access article distributed under the terms of the Creative Commons Attribution-NonCommercial-NoDerivatives License (<http://creativecommons.org/licenses/by-nc-nd/4.0/>), which permits non-commercial re-use, distribution, and reproduction in any medium, provided the original work is properly cited, and is not altered, transformed, or built upon in any way.

Table 1. List of *Spiniferites* taxa in the reference modern database of the Northern Hemisphere (n = 1490) that are used here for statistical purpose, with summary information about their occurrence.

Name	Number of sites (nb)	Maximum %	nb > 0.5%	nb > 1%	nb > 10%
<i>Spiniferites beherius</i>	91	4.9	62	46	0
<i>Spiniferites bentorii</i>	89	10.8	71	58	2
<i>Spiniferites bulloideus</i>	108	6.3	56	40	0
<i>Spiniferites delicatus</i>	157	57.8	104	76	14
<i>Spiniferites elongatus</i>	1038	48.0	907	746	60
<i>Spiniferites lazus</i>	52	2.2	22	8	0
<i>Spiniferites membranaceus</i>	73	23.4	42	24	5
<i>Spiniferites mirabilis-hyperacanthus</i>	396	77.0	289	208	87
<i>spiniferites pachydermus</i>	1	0.3	0	0	0
<i>Spiniferites ramosus</i>	938	40.4	808	635	66
<i>Spiniferites</i> spp.	912	23.9	698	483	35
<i>Spiniferites</i> spp. granular	55	5.7	42	32	0

Table 2. Morphological features used to distinguish the main *Spiniferites* taxa in the reference database.

	Central body	Processes	Sutural crests	Species	
Proximo-chorate cysts with sutural processes	Pear-shaped with apical boss	Occasional intergonal	Low	<i>S. bentorii</i>	
		Abundant intergonal	Low, but broad antapical flange with intergonal processes	<i>S. mirabilis</i>	
	Sphaerical to Sub-sphaerical	Occasional intergonal	Low	<i>S. hyperacanthus</i>	
		Rare intergonal	Moderate, and well developed between gonal antapical processes	<i>S. membranaceus</i>	
	Ovoidal	Gonal only	Irregular processes	Septa developed mostly on the hypocyst	<i>S. beherius</i>
			Processes membranous with petaloid tips	High sutural crests	<i>S. delicatus</i>
		Process base large and fenestrate	Moderate sutural crests	<i>S. lazus</i>	
	Elongate	Gonal only	Processes short to long well defined terminal furcations	Moderate sutural crests	<i>S. bulloideus</i> <i>S. ramosus</i>
			Processes shorter in circular area	Sutural septa well developed at the apex and antapex	<i>S. elongatus</i>

researchers present their results after grouping specimens of *Spiniferites* at genus level. In order to deal with this issue, we developed an “operational taxonomy” with the aim to establishing standardized databases. The operational taxonomy is based on the definition of visually explicit taxa categories used for identification during routine observation and counting of dinocysts in optical microscopy under transmitted light at magnification of 400X to 1000X (Rochon et al. 1999; de Vernal et al. 1997, 2001, 2005, 2013; Bonnet et al. 2012). It thus requires morphological features clearly recognisable under optical microscope. In many cases, it results in the grouping of taxa that visually constitute a morphological continuum. The use of an operational taxonomy is a compromise. However, it is useful for systematic counts undertaken with the aim of statistical population analyses and quantitative palaeoecological studies, including the application of transfer functions or modern analogue techniques (Guiot & de Vernal 2007).

Here, we examine the distribution of the main *Spiniferites* taxa occurring in surface sediments of the Northern Hemisphere as reported in the most recent standardized dinocyst database (de Vernal et al. 2013). We first provide an overview of the operational taxonomy used to develop the database including the *Spiniferites* taxa and we report on the spatial distribution of the taxa and their relationships with sea-surface temperature and salinity, in both winter and

summer, sea ice cover, primary productivity, bathymetry and distance to the coast. The objective of this work is to assess the ecological significance and usefulness of the main taxa in spite of taxonomical uncertainties and, therefore, to provide clues for a sound use of *Spiniferites* in qualitative and/or quantitative palaeoecological, palaeoceanographical and palaeoclimatic investigations.

2. Material and methods

2.1. The dinocyst data and the taxonomical status of *spiniferites* taxa

The standardized dinocyst database of the Northern Hemisphere was first developed in the 1990s with the aim to make transfer functions and/or to apply modern analogue techniques for quantitative palaeoceanographical reconstructions. The earliest works using the proto-database, which included mainly samples from the northwest North Atlantic and adjacent seas, were published in de Vernal et al. (1992a, 1993). Following this pioneering work, the enlargement of the database with samples from the Norwegian Sea was undertaken by adopting a systematic approach with regard to standardized palynological preparation techniques, implying treatments with warm hydrofluoric and hydrochloric acids but no oxidation, and sieving at 10 µm. The database

was developed using an operational taxonomy established after several workshops and reported in Rochon et al. (1999). Updates of the database using the same taxonomy were published using the studies by Radi & de Vernal (2004, 2008), Radi et al. (2007), Pospelova et al. (2008), Vasquez-Bedoya et al. (2008), Limoges et al. (2010) and Bonnet et al. (2012). Despite enlargement of the geographic coverage and taxonomic refinements, the list of *Spiniferites* taxa has remained the same since the initial versions of the reference database. In the last published update of the database, a total of 66 dinocyst taxa were reported including 12 *Spiniferites* taxa after grouping (de Vernal et al. 2013). The same database was used here with the exception of two sites and the grouping was not exactly the same. Hence, the data set reported in this manuscript comprises 1490 sites with counts for 67 taxa, including 12 *Spiniferites* categories. (Table 1) The entire data set is available online on the Geotop website (www.geotop.ca).

The general identification criteria for *Spiniferites* cysts distinguish light transparent specimens with a rounded to elongate body, where a Gonyaulacoid tabulation is distinct due to developed sutural ridges and numerous surrounding multifurcate processes in gonial and sometimes in intergonial position. Among these taxa, some have a morphology that permits unquestionable identification whereas others have more subtle characteristics making unequivocal assignment more uncertain, as briefly exposed below in alphabetical order of the species names (see also Table 2; Plates 1–3). More details about the taxonomical affinities of *Spiniferites* taxa and their morphological characteristics can be found in the reports published in this volume by Limoges et al., Londeix et al., Mertens et al. and Van Nieuwenhove et al.

Spiniferites belerius Reid 1974 (Plate 3) is a small cyst with an ovoidal central body and smooth surface, gonial and occasionally intergonial processes of irregular shape, and low sutural crests. *Spiniferites belerius* can bear processes of variable shapes and membranous septa between processes may develop, notably at the antapex (cf. Harland 1977; Rochon et al. 1999). The development of an antapical septum is also characteristic of *Spiniferites membranaceus* (Rossignol 1964) Sarjeant 1970 (see below and Plate 3). *Spiniferites belerius* and *Spiniferites membranaceus* were grouped together in an earlier version of the database (Rochon et al. 1999), but not here. Although *Spiniferites belerius* was counted as a distinct species, its morphological characteristics are a matter of discussion (Mertens et al. 2018). We cannot exclude the possibility that specimens of *Spiniferites belerius* were included in the *Spiniferites* spp. during routine counts. Therefore, caution is required when using the proportion of this taxon for quantitative purpose.

Spiniferites bentorii (Rossignol 1964) Wall & Dale 1970 (Plate 2) is easily distinguishable from other species based on its large pear-shaped central body, microgranular surface, relatively thick wall, and a pronounced apical boss (e.g. Rochon et al. 1999). Beyond these general characteristics, specimens assigned to *Spiniferites bentorii* may show morphological variations with regard to the length of processes, which are usually short, and with the shape of the processes,

from conical to tapering and erect to curved (cf. Harland 1977). Moreover, intergonial processes can occur occasionally, as reported by Limoges et al. (2018).

Spiniferites bulloideus (Deflandre & Cookson 1955) Sarjeant 1970 (Plate 3) is a small sub-spherical cyst with smooth wall surface, no apical boss, low sutural crests and bearing exclusively gonial processes. *Spiniferites bulloideus* is very similar to *Spiniferites ramosus* (Ehrenberg 1837b) Mantell 1854 (see also Mertens et al. 2018 and Londeix et al. 2018). *Spiniferites bulloideus* was considered to be a junior synonym of *Spiniferites ramosus* by Harland (1977). In the reference database, *Spiniferites bulloideus* was counted independently. However, many researchers agree on the difficulty to distinguish *Spiniferites bulloideus* in routine counts and tend to group them with *Spiniferites ramosus* or *Spiniferites* spp.

Spiniferites delicatus Reid 1974 (Plate 2) is characterized by membranous sutural crests and gonial processes with petaloid process tips. Its ovoidal central body sometimes bears a low apical boss. There are microgranulations on the outer wall layer, on the processes and sutural crests. *Spiniferites delicatus* is easy to distinguish from other *Spiniferites* taxa in the database. However, it might include *Spiniferites ristingensis* Head 2007, which is very similar (Mertens et al. 2018) and was described by Head (2007) from Eemian sediments of the Baltic Sea. *Spiniferites delicatus* was a minor component of assemblages in the early versions of the database, which included mostly cool temperate to polar North Atlantic sites (de Vernal et al. 1997; Rochon et al. 1999). In the most recent versions of the database that include samples from low latitudes (Vasquez-Bedoya et al. 2008; Limoges et al. 2010) it became an important taxon.

Spiniferites elongatus Reid 1974 (Plate 1) comprises all *Spiniferites* cysts having a conspicuously elongate cyst body and variably developed septa in the apical and antapical zones. *Spiniferites elongatus* as described by Reid (1974) has a smooth to finely microgranulate surface, exclusively gonial processes, and membranous hollow sutural septa varying in height, from low around the cingulum to high at the apex and antapex. Later observations showed that the height of sutural septa and their degree of development in these elongate *Spiniferites* cysts is very variable. At the end member, specimens with particularly extensive development of the membranous sutural septa and less prominent processes were assigned to *Spiniferites frigidus* described by Harland and Reid and/or *Rottnestia amphicavata* described by Dobell and Norris, both from recent Beaufort Sea sediments, in Harland et al. (1980). Synonymy between *Spiniferites frigidus* and *Rottnestia amphicavata* was proposed by Bujak (1984). However, in the systematic section of Rochon et al. (1999), Head recommended to maintain the species status of *Rottnestia amphicavata* arguing that it represents a distinct end member, notably because of the discrete structure of processes usually recognized only by presence of their distal furcations surmounting sutural septa in gonial position. More recently, it was suggested that both *Spiniferites frigidus* and *Rottnestia amphicavata* are junior synonyms of *Spiniferites elongatus* (Van Nieuwenhove et al. 2018). The main arguments in favor of synonymy are the

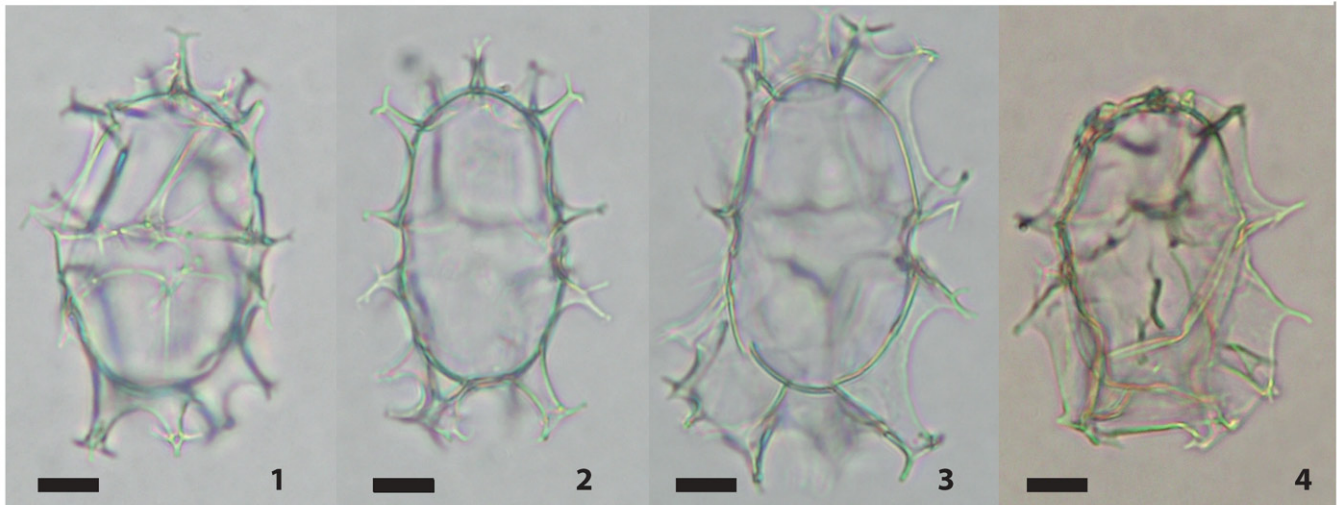
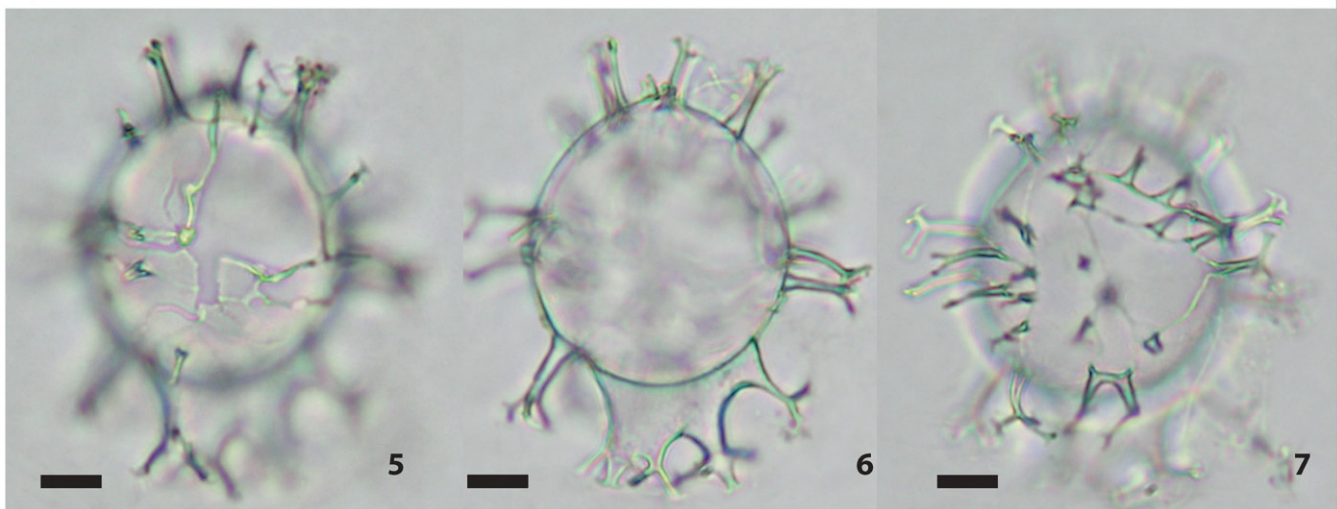
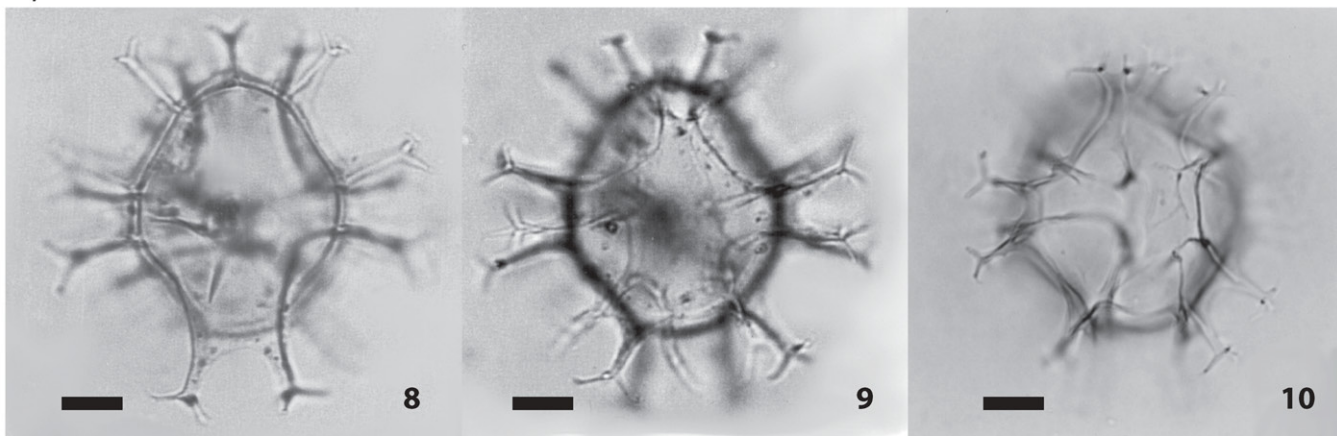
Spiniferites elongatus*Spiniferites mirabilis**Spiniferites ramosus*

Plate 1. 1–4. Different specimens of *Spiniferites elongatus* (photos from AR, Gulf of St. Lawrence): continuum from *Spiniferites elongatus* (1) to morphotypes formerly assigned to *Spiniferites frigidus*/*Rottnestia ampicavata* (now *Spiniferites elongatus* – Beaufort morphotype) (4), central body length from 40 to 50 μm ; 5–7. *Spiniferites mirabilis* (photos from AR, Gulf of St. Lawrence) in dorsal (5) and ventral (7) views and optical section (6), central body diameter 60 μm . 8–9. *Spiniferites ramosus* (figured in de Vernal & Mudie 1989; Labrador Sea) in dorsal (8) and ventral (9) views, central body length 40 μm . 10. *Spiniferites ramosus* (figured in Rochon et al. 1999; western North Atlantic) in ventral view, central body length 40 μm . All scale bars = 10 μm .

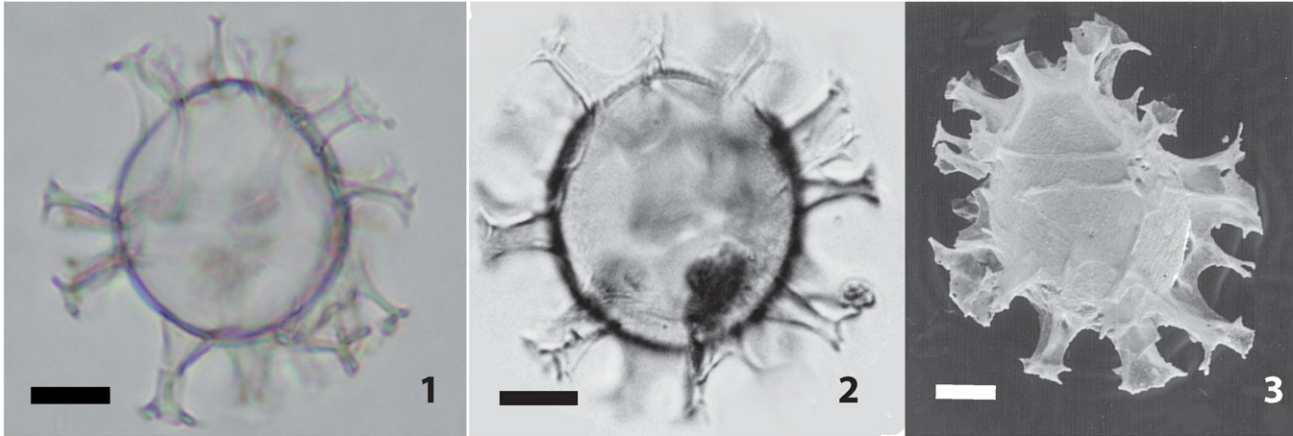
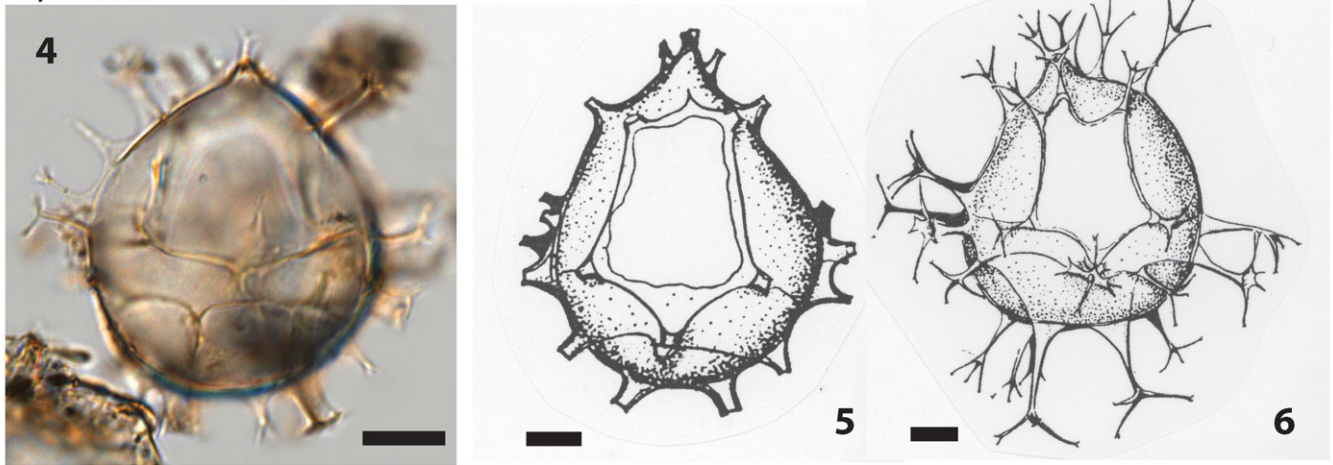
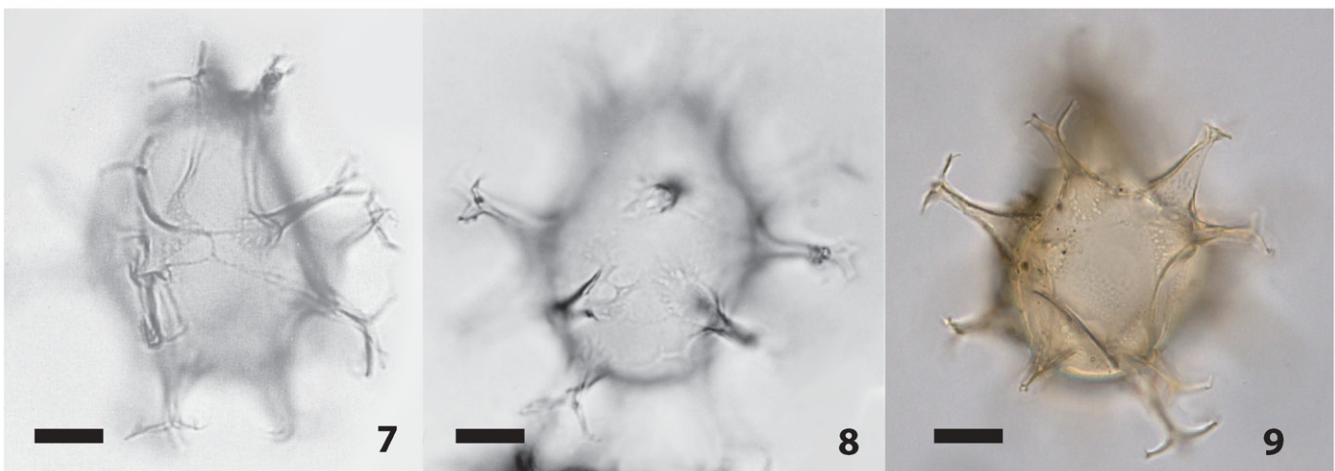
Spiniferites delicatus*Spiniferites bentorii**Spiniferites lazus*

Plate 2. 1–3. Different specimens of *Spiniferites delicatus* in optical microscopy (1 Photo from AR; Gulf of St. Lawrence. 2 figured in Rochon et al. 1999; Western Mediterranean Sea) and scanning electron microscopy (3 figured in Turon & Londeix 1988; Western Mediterranean Sea), central body length 38–40 μm . 4–6. *Spiniferites bentorii* in optical microscopy (4 figured in Limoges et al. 2013; Gulf of Mexico) and original drawings (4–5) of the type species by Rossignol (1964) from the Mediterranean Sea, central body length 45 μm (4) and 60 μm (5–6). 7–9. Different specimens of *Spiniferites lazus* (7–8 figured in Rochon et al. 1999; North Sea; 9 photo from NVN, Iceland Plateau, North Atlantic Ocean), central body length 45 μm . All scale bars = 10 μm .

fact that there is a continuum between *Spiniferites elongatus* and that the morphological end-members were originally defined as *Spiniferites frigidus*/*Rottneusia ampicavata*

without clear criteria to separate the entities for routine population counts (cf. Rochon et al. 1999; Heikkilä et al. 2014; Van Nieuwenhove et al. 2018). However, the latter

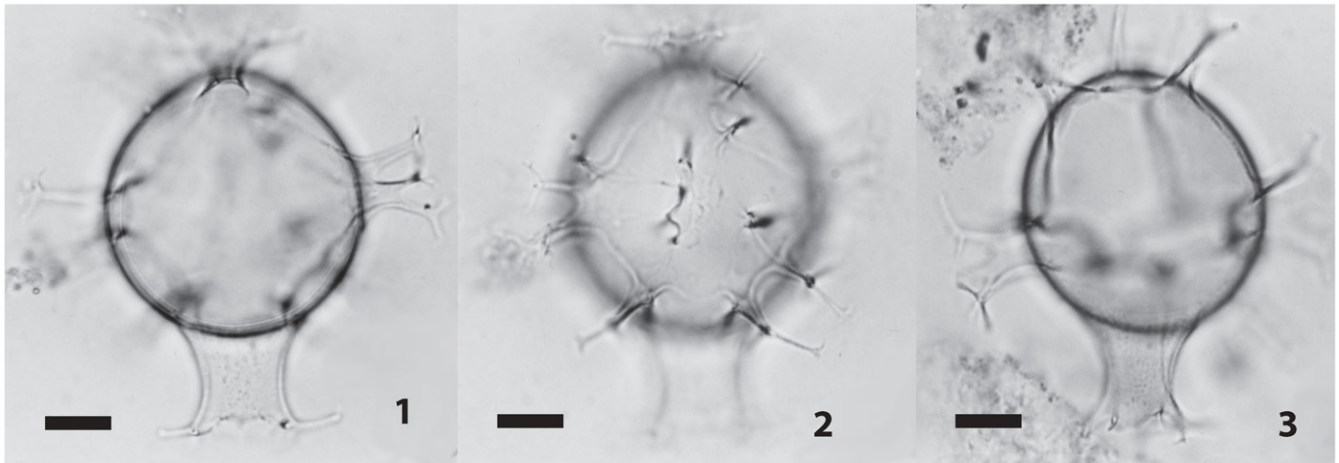
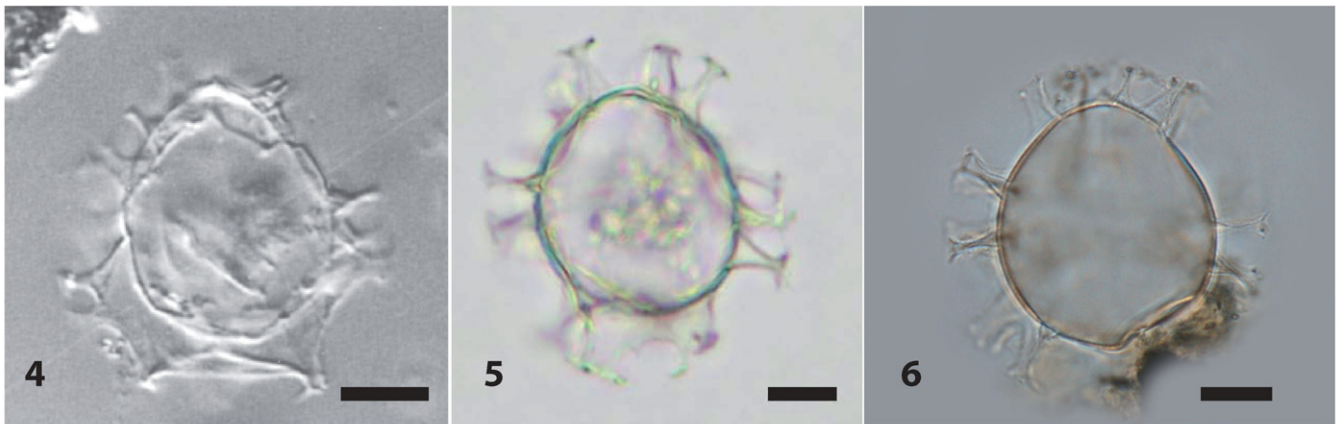
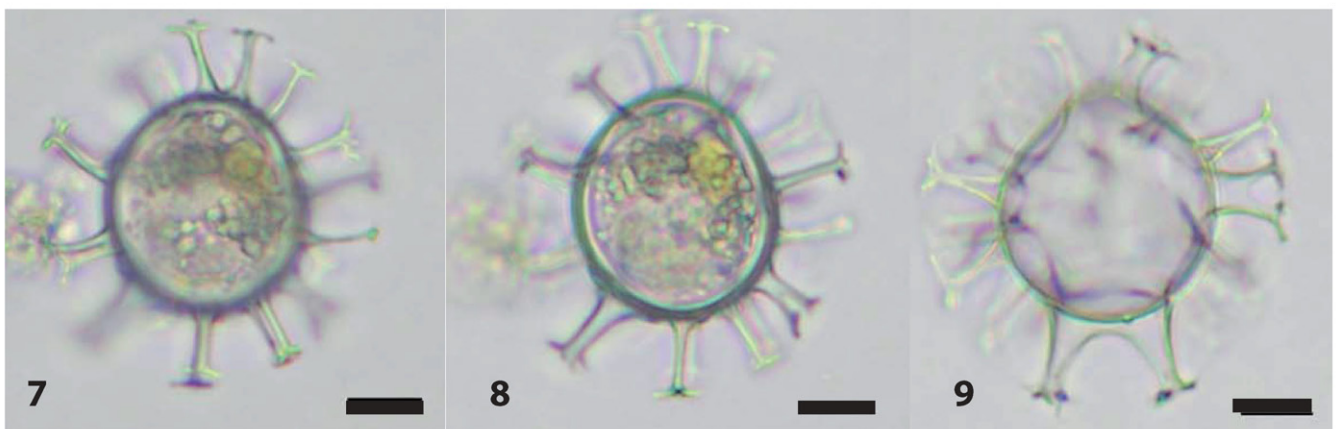
Spiniferites membranaceus*Spiniferites belerius**Spiniferites bulloideus*

Plate 3. 1–3. *Spiniferites membranaceus* (figured in Rochon et al. 1999; North Sea), central body length 46 μm . 4–6. Different specimens of *Spiniferites belerius* in optical microscopy (4 figured in de Vernal et al. 1992b; Western Mediterranean Sea; 5 Photo from AR; Gulf of St. Lawrence; 6 Photo from VP; East China Sea). 7–9. *Spiniferites bulloideus* in optical microscopy (photos from AR; Gulf of St. Lawrence). All scale bars = 10 μm .

authors introduced an informal type, *Spiniferites elongatus* – Beaufort morphotype, to refer to specimens with the extreme morphology formerly attributed to *Spiniferites frigidus* or *Rottnestia ampicavata*. Hence, all these morphologies are herein simply referred to as *Spiniferites elongatus*, corresponding to the grouping under *Spiniferites elongatus*

sensu lato that has been used in most publications dealing with the Quaternary palaeoceanography of cool temperate to subarctic seas.

Spiniferites lazus Reid 1974 (Plate 2) has an ovoidal central body with microgranular to microreticulate surface, and very often a small apical boss. The processes are exclusively gonal

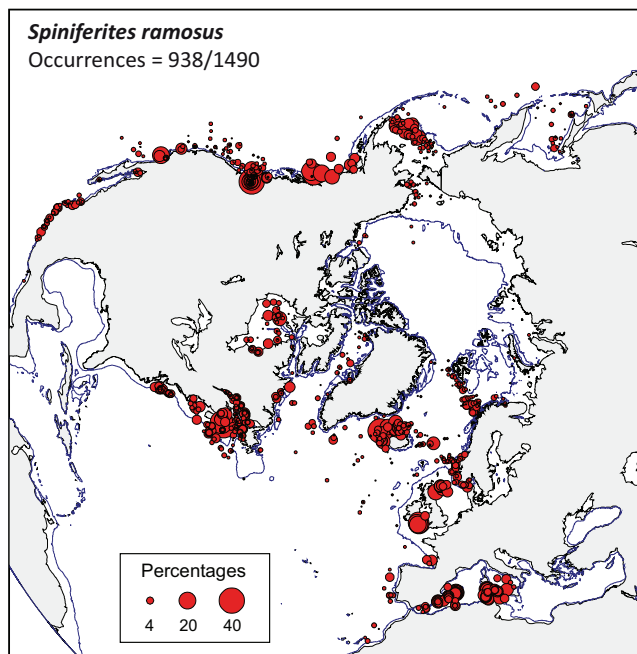


Figure 1. Distribution of *Spiniferites ramosus* in the $n = 1490$ database: (a) Map of relative abundance in percentages relative to total dinocyst counts and (b) graphs of percentage vs. sea-surface temperature in winter and summer, sea-surface salinity in winter and summer, sea-ice cover, productivity, bathymetry and distance to the coast. In the map, the isobath corresponds to 200 meters of water depth. Source: figures drafted by the authors using MapInfo.

and are distally furcate with recurved bifurcate tips and the sutural crests are low. The distinctive feature of *Spiniferites lazus* is the fenestration on the expanded process bases (cf. Rochon et al. 1999). *Spiniferites lazus* is easy to distinguish, but is rarely abundant in the modern database.

Spiniferites membranaceus (Rossignol 1964) Sarjeant 1970 (Plate 3) has an ovoidal central body without apical boss. The processes are exclusively gonial and are distally furcate with recurved bifurcate tips. Sutural crests are low, except on the dorsal side of the antapex, where they form a conspicuous membrane. The well-developed antapical septa are a feature that permits distinction from *Spiniferites ramosus*.

Spiniferites mirabilis (Rossignol 1964) Sarjeant 1970 (Plate 1) is a taxon recording large morphological variations. It is typically characterized by a large spheroidal to sub-spheroidal central body, low to absent sutural crests, the presence of gonial and intergonial processes and a conspicuous flange linking gonial and intergonial processes at the antapex. Beyond this general description, *Spiniferites mirabilis* may display important variations in the ornamentation of the outer wall from smooth to densely microgranular, the development of sutural crests, the number and height of intergonial processes, including those making up the antapical flange, and the presence/absence of an antapical boss (cf. Limoges et al. 2018). With the exception of the antapical flange, the same characteristics and ranges of variations apply to *Spiniferites hyperacanthus* (Deflandre & Cookson 1955) Cookson & Eisenack 1974. Because the orientation of the cysts or folding may prevent observation of the antapical zone to see the flange, *Spiniferites mirabilis* and *Spiniferites hyperacanthus* are grouped together as *Spiniferites mirabilis-hyperacanthus*. The morphology and taxonomic affinities of *Spiniferites*

Spiniferites ramosus
N = 938

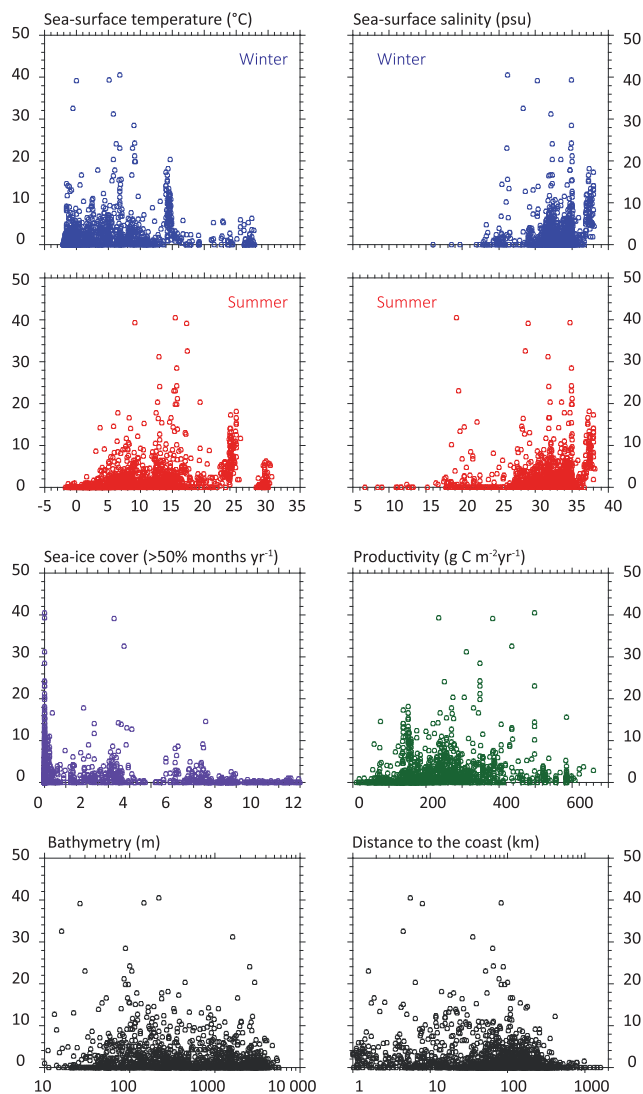


Figure 1. Continued.

hyperacanthus, which was described from Miocene deposits, are discussed with more details by Londeix et al. (2018).

Spiniferites ramosus (Ehrenberg 1837b) Mantell 1854 (Plate 1) is one of the most commonly recorded *Spiniferites* species. Under this name, there are very variable morphologies, which led to the description of many subspecies ($n = 32$; Williams et al. 2017). The main characteristic of the ovoid cyst is to exclusively bear gonial processes, have a smooth wall surface and no apical boss. Sutural crests are low but more developed towards the processes (cf. Rochon et al. 1999). Normally, the processes are long, often hollow at their base with distal trifurcations having bifurcate tips. However, the length of the processes is highly variable and the morphology of their distal ends is not always well expressed (e.g. Lewis et al. 1999). Moreover, there is occasional development of narrow trabeculae between adjacent process tips. In some (perhaps teratologic) cases, the trabeculae are well developed and form a network (e.g. Rochon et al. 2009), which may lead to confusion with *Nematosphaeropsis labyrinthus* (Ostenfeld 1903) Reid 1974 or *Nematosphaeropsis rigida*

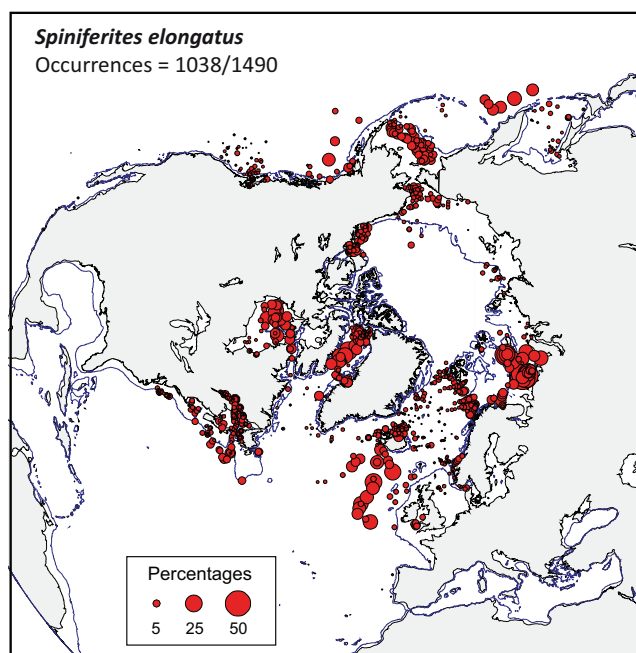


Figure 2. Distribution of *Spiniferites elongatus* in the $n = 1490$ database: (a) Map of relative abundance in percentages relative to total dinocyst counts and (b) graphs of percentage vs. sea-surface temperature in winter and summer, sea-surface salinity in winter and summer, sea-ice cover, productivity, bathymetry and distance to the coast. In the map, the isobath corresponds to 200 meters of water depth. Source: figures drafted by the authors using MapInfo.

Wrenn 1988. *Spiniferites bulloideus* is morphologically very similar to *Spiniferites ramosus* but it is more spherical, smaller, and more delicate in structure than the typical *Spiniferites ramosus* (Harland 1977). Hence, *Spiniferites bulloideus* has been treated as a junior synonym of *Spiniferites ramosus* (Harland 1977) and is often grouped with *Spiniferites ramosus*. In recent sediments, *Spiniferites ramosus* is one of the most commonly reported taxa of the genus, but its taxonomical identification is very lax as large morphological variations are usually accepted. For typical specimens (i.e., Plate 1, figures 8-9), we may recommend to use the name *Spiniferites ramosus* subsp. *ramosus* and to use *Spiniferites ramosus* sensu lato for other morphologies of the species, including *Spiniferites bulloideus*.

Spiniferites pachydermus (Rossignol 1964) Reid 1974 is a large ($>50\mu\text{m}$) spherical to subspherical cyst often with a low apical boss, low sutural crests and gonal trifurcate processes, which is distinguished by a very thick ($\sim 3\mu\text{m}$) microgranulate to fibrous wall (cf. Reid 1974; cf. also Londeix et al. 2018). The diagnostic criteria of *Spiniferites pachydermus* are discussed by Mertens et al. (2018). *Spiniferites pachydermus* was reported only once in the database.

Spiniferites spp. is a category often used to group specimens of *Spiniferites* that are not identified at species level because of unsuitable orientation, folding or poor preservation, or because ambiguous characteristics make its unequivocal assignment to species level difficult. This category also corresponds to specimens belonging to undescribed species or to species occurring rarely and not yet introduced in the standardized database. Hence, *Spiniferites* spp. is a wide category without precise significance. It should

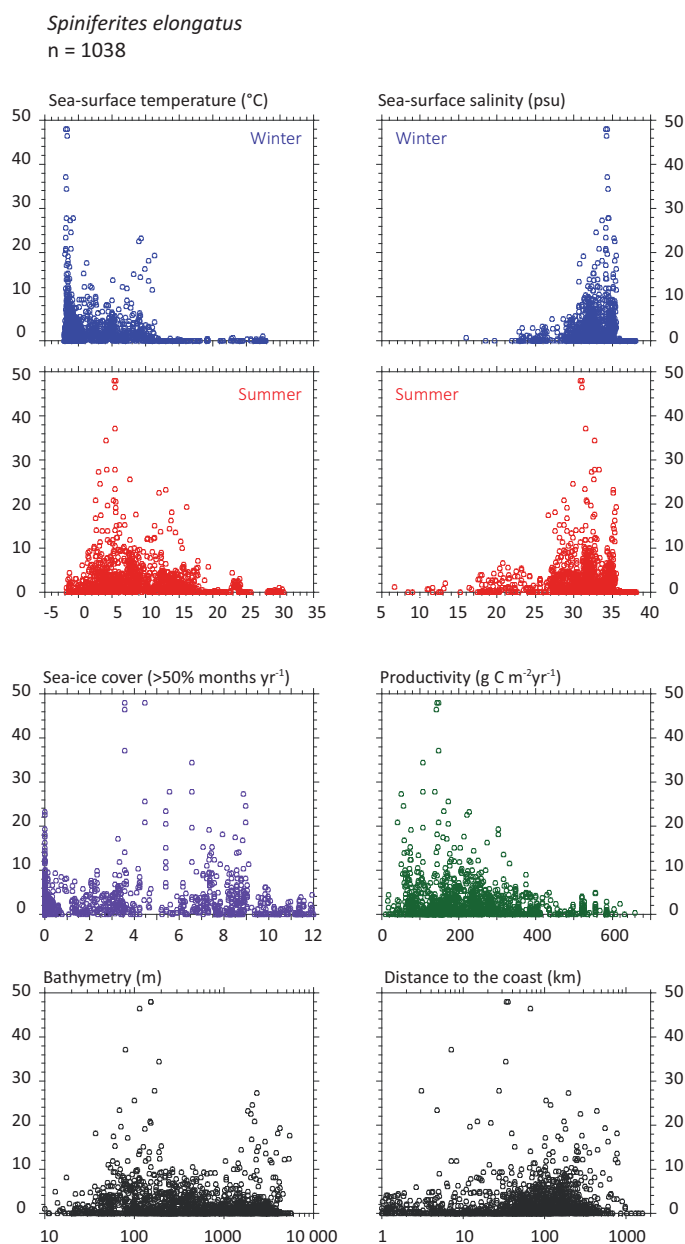


Figure 2. Continued.

not be used for ecological purpose, except as being an indicator of taxonomic diversity.

Spiniferites spp. granular is an informal name for all *Spiniferites* specimens with gonal processes and a thick ($\sim 1\mu\text{m}$) and granular outer wall. The specimens assigned to *Spiniferites* spp. granular have variable sizes and morphologies, the only common feature being the relatively thick granular wall. The nomenclature of this informal taxonomic category is questionable as discussed by Londeix et al. (2018). *Spiniferites* spp. granular is mentioned here but not used for ecological inference.

2.2. The environmental data

The surface sediment samples used to develop the dinocyst database were collected in nearshore to offshore sites and are representative of estuarine, coastal, neritic and oceanic

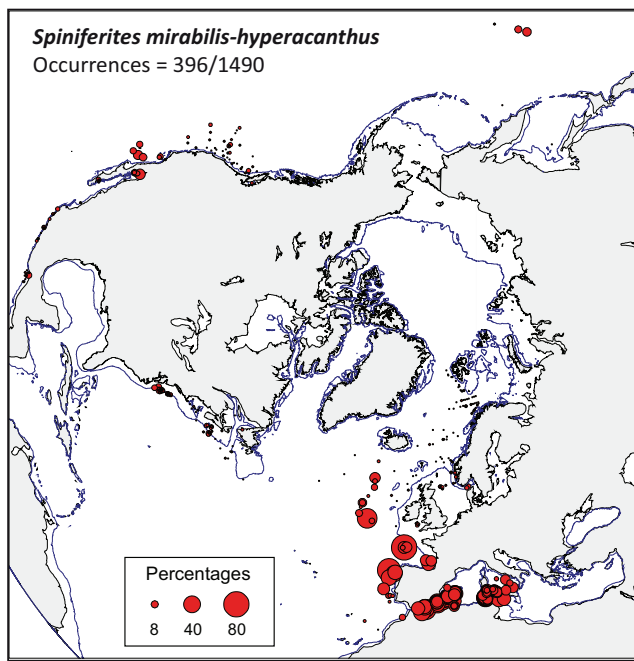


Figure 3. Distribution of *Spiniferites mirabilis-hyperacanthus* in the $n = 1490$ database: (a) Map of relative abundance in percentages relative to total dinocyst counts and (b) graphs of percentage vs. sea-surface temperature in winter and summer, sea-surface salinity in winter and summer, sea-ice cover, productivity, bathymetry and distance to the coast. In the map, the isobath corresponds to 200 meters of water depth. Source: figures drafted by the authors using MapInfo.

conditions. The environmental data compiled here include sea-surface temperature (SST), salinity (SSS), sea ice cover and primary productivity in addition to the bathymetry and distance from the coast. Sea-surface temperature (SST) and salinity (SSS) were compiled from the 2001 version of the World Ocean Atlas (cf. Conkright et al. 2002). The mean February, August, winter (January–February–March) and summer (July–August–September) SSTs and SSSs were calculated from values collected within a radius of 30 nautical miles around each station. The sea-ice cover data were compiled on a 1×1 degree grid scale based on data spanning 1953–2003, which were provided by the National Snow and Ice Data Center (NSIDC) in Boulder. We express sea ice as the number of months per year of sea ice with concentration $>50\%$, which correlates with the mean annual concentration (cf. de Vernal et al. 2013). The primary productivity data are from satellite observation of water properties of the oceans as calculated with the Vertical Generalized Production Model (VGPM) described by Behrenfeld & Falkowski (1997). The data used here have a spatial resolution of 4.63 km and were provided by the MODerate resolution Imaging Spectroradiometer (MODIS) program. MODIS was launched by the National Aeronautics and Space Administration (NASA) in 2000 (cf. Radi & de Vernal 2008). Primary productivity is referred as productivity for the remainder of this text. The bathymetry and the distance to the coastline were calculated mostly from the 2014 version of the General bathymetric map of the ocean (GEBCO) in addition to complementary information from the European Marine Observation and Data Network (EMODnet) and the

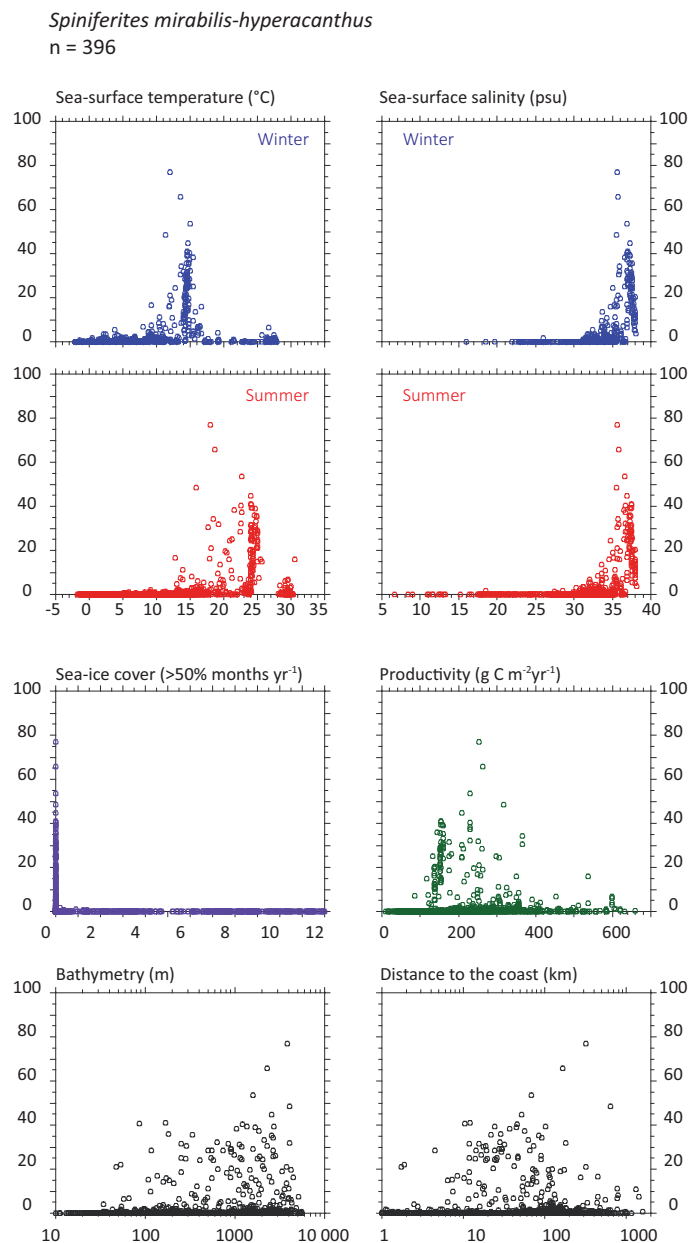


Figure 3. Continued.

International Bathymetric Chart of the Arctic Ocean (IBCAO) for the European margins and Arctic, respectively.

The sample sites cover a wide domain of SSTs, which range from freezing to 30.6°C . They also cover a wide domain of SSSs, which range from 7 to 38 psu. SSS and SST of both winter and summer were considered in addition to SST and SSS of February and August, which are typically the coldest and warmest months of the year. The data set includes a large number of sites ($n = 774$) marked by the occurrence of sea ice for more than 0.1 monthly^{-1} and many sites are characterized by contrasted SSTs in summer and winter. The seasonal duration of sea ice, which is proportional to the mean annual concentration, is a very important parameter of the data set as it determines the life cycle of the biota (e.g., Vancoppenolle et al. 2013).

The parameters ($n = 13$) used for quantitative data treatments are listed in Table 3 and the corresponding values

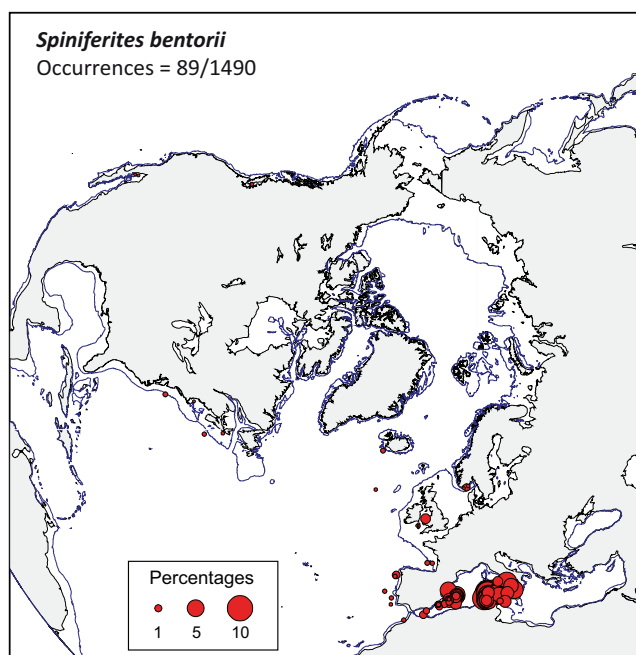


Figure 4. Distribution of *Spiniferites bentorii* in the $n = 1490$ database: (a) Map of relative abundance in percentages relative to total dinocyst counts and (b) graphs of percentage vs. sea-surface temperature in winter and summer, sea-surface salinity in winter and summer, sea-ice cover, productivity, bathymetry and distance to the coast. In the map, the isobath corresponds to 200 meters of water depth. Source: figures drafted by the authors using MapInfo.

at the 1490 sites can be found on the Geotop website. Among selected parameters, the hydrographic factors such as seasonal temperature and salinity in addition to sea ice cover are critical as they are used for applications in palaeoclimatology and palaeoceanography. Productivity, bathymetry and distance to the coast are important too, but more from an ecological or taphonomical point of view. There are other parameters likely playing a role on the distribution of dinoflagellates and their cysts, and they may include turbulence, water mass stratification, competition with primary producers, sedimentation rates and selective preservation of organic compounds, etc. In-between site comparison of seasonal, annual, and inter-annual *Spiniferites* cyst production in eight sediment traps from different geographic regions highlights that such parameters are not easily available or quantifiable although their importance increases in highly heterogeneous estuarine systems (Pospelova et al. 2018).

2.3. The data treatments

In the database, the average sum of dinocysts counted is 356 (minimum 60 and maximum 4012) and the total number of taxa is 67, including 12 *Spiniferites* categories (see Table 1). The relative occurrences or percentages of *Spiniferites* taxa were calculated vs. the total dinocyst count (cf. Figures 1–8). Multivariate analyses were conducted from the percentages of *Spiniferites* taxa vs. the sum of total dinocysts (Figure 9) and also vs. the sum of *Spiniferites* cysts only in

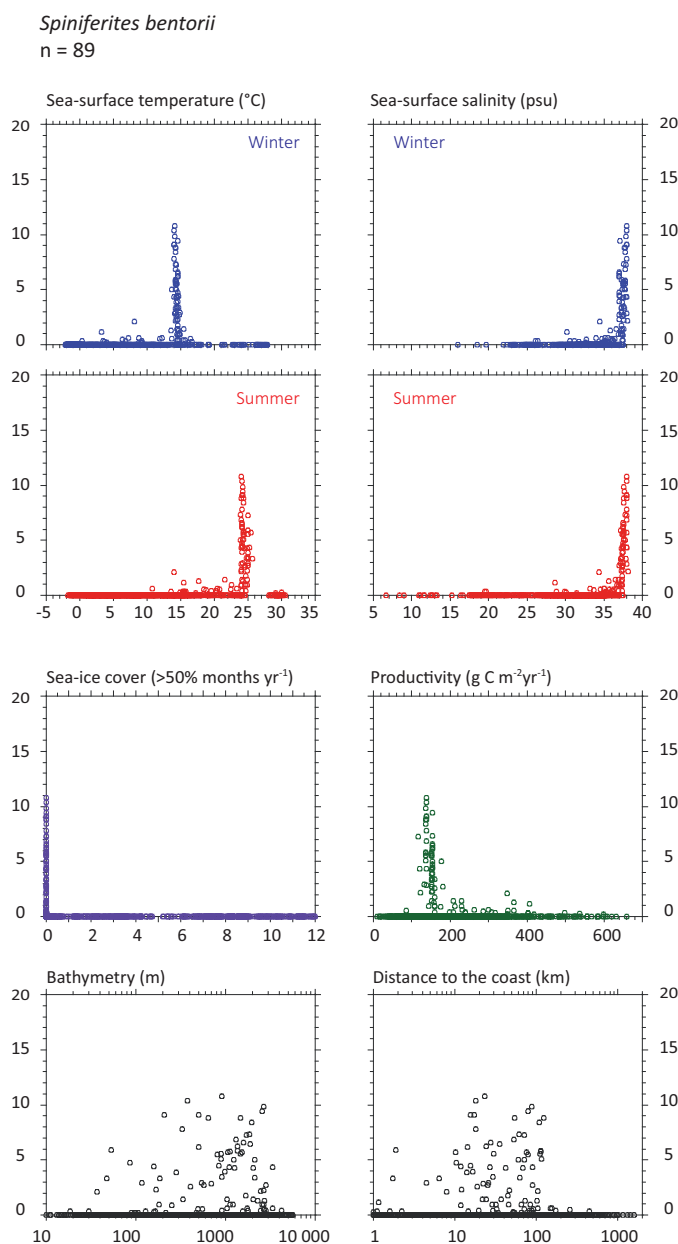


Figure 4. Continued.

order to emphasize the significance of the taxa within the *Spiniferites* group (Figure 10).

The multivariate analyses were performed with the Canoco software version 4.5 (Ter Braak & Smilauer 2002) on the taxa distribution and sea-surface conditions in the $n = 1490$ database after logarithmic transformation of relative percentages of dinocyst taxa. The transformation aims at giving more weight to accompanying taxa, which can be more diagnostic of environmental conditions than the dominant taxa that are often cosmopolitan (cf. for ex. de Vernal et al. 2001).

Detrended correspondence analyses (DCA) were first performed to identify the type of function between assemblages and environmental variables (cf. Ter Braak & Smilauer 2002). When taking into account the 1490 sites, 66 taxa and 13 environmental parameters, the results show that the length of the first axis (2 standard deviations) is close to 4, which

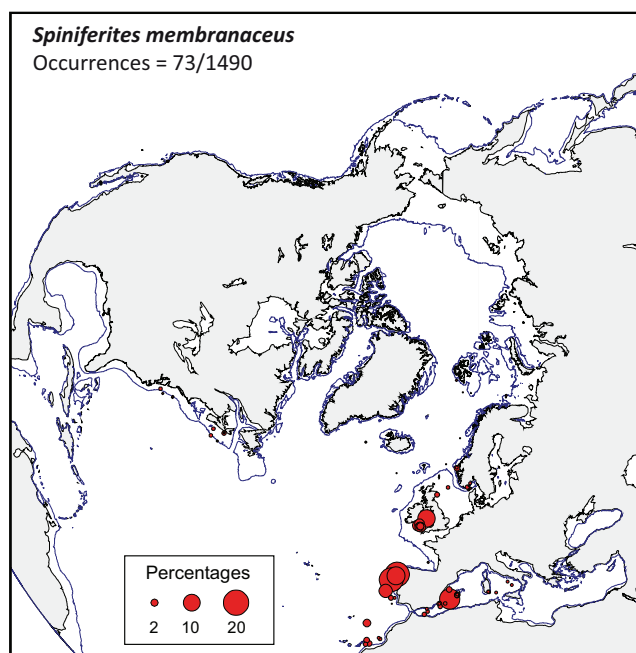


Figure 6. Distribution of *Spiniferites membranaceus* in the $n = 1490$ database: (a) Map of relative abundance in percentages relative to total dinocyst counts and (b) graphs of percentage vs. sea-surface temperature in winter and summer, sea-surface salinity in winter and summer, sea-ice cover, productivity, bathymetry and distance to the coast. In the map, the isobath corresponds to 200 meters of water depth. Source: figures drafted by the authors using MapInfo.

ecological affinities, unlike what was suggested in Rochon et al. (1999).

Spiniferites mirabilis-hyperacanthus (Figure 3) occurs in low numbers in many samples but may reach very high percentages (>10% and up to 80%) in offshore areas where relatively high SSTs (10–15 °C in winter; >18 °C in summer) and SSSs (>35 psu) are recorded. It is abundant in the North Atlantic in the vicinity of the Gibraltar Strait and in the north-eastern sector of the subtropical gyre.

Spiniferites bentorii (Figure 4) occurs in a small number of samples and with low percentages, rarely exceeding 10%. In the database, the maximum abundance of *Spiniferites bentorii* is recorded in the Algerian and Tyrrhenian basins of the western Mediterranean Sea where SSTs (13–15 °C in winter, 23–25 °C in summer) and SSSs (>36 psu) are high, but productivity is low (<150 gC m⁻²y⁻¹).

Spiniferites delicatus (Figure 5) is a neritic taxon that gained importance in the Northern Hemisphere database with the addition of low-mid latitudes samples (e.g. Vasquez-Bedoya et al. 2008; Limoges et al. 2010). It occurs in relatively high percentages (>5%) in warm-temperate to tropical environments (SSTs ranging 25–30 °C) and shows preference for low seasonal contrasts of SST and SSS around 34 psu.

Spiniferites membranaceus (Figure 6) occurs mostly along the southwest European margins off the Eastern Atlantic coasts and western Mediterranean Sea. It is rarely abundant, with low number of sites recording >5%. At the few sites where it is relatively abundant, it shows affinities for saline (>34) environments with a wide SST range (from 6 °C in winter to 26 °C in summer), and productivity (up to 400 gC m⁻²y⁻¹).

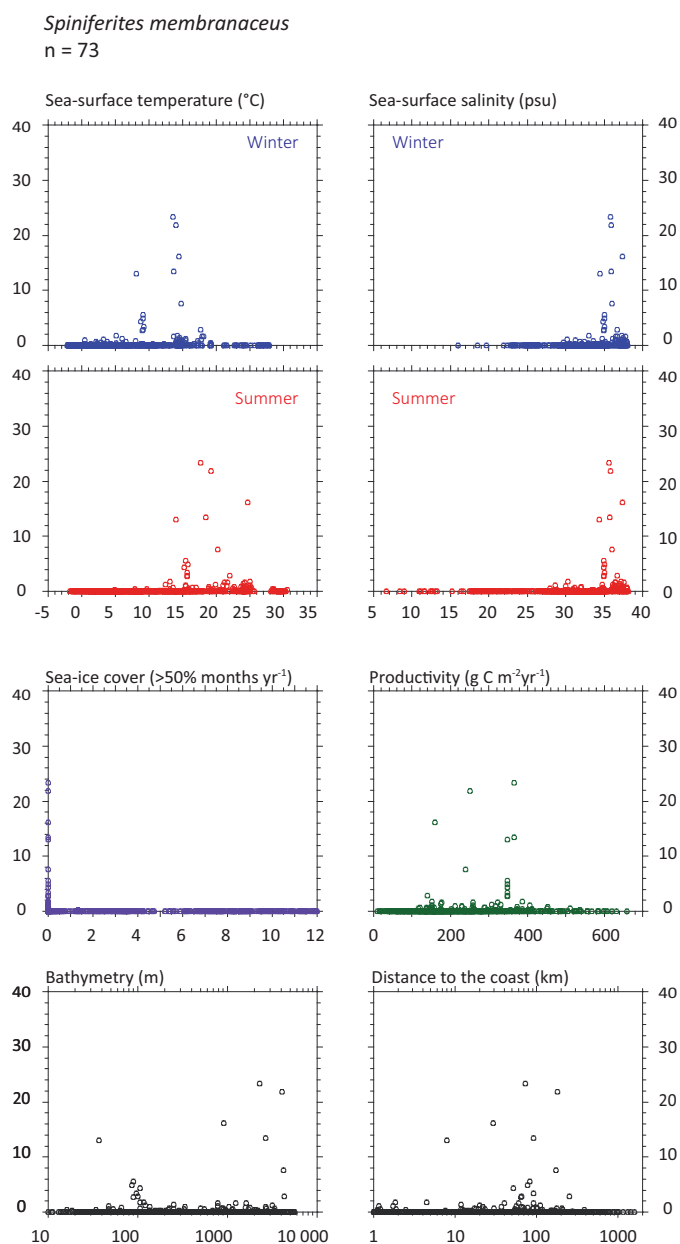


Figure 6. Continued.

Spiniferites lazus (Figure 7) occurs only at a few sites of the modern database and it is rarely more abundant than 2%. The data show that *Spiniferites lazus* occurs in temperate areas (cool in winter and up to 25 °C in summer) where salinity is relatively high and productivity variable (up to 500 gC m⁻²y⁻¹) is recorded.

3.2. Summary of spiniferites taxa distribution in the hydrographical space

Beyond the distribution of individual taxa (Figures 1 – 7), a summary figure of the distribution of key species was built from the mean summer SSS and SST corresponding to the occurrences from low (>0.5%) to relatively high relative occurrences (>5% or >10%; see Figure 8 and Table 3). Figure 8 shows that *Spiniferites ramosus* has a very wide

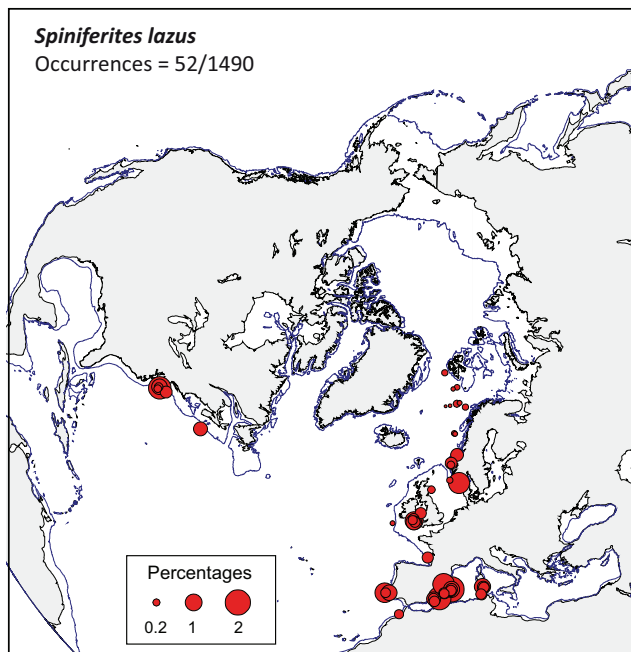


Figure 7. Distribution of *Spiniferites lazus* in the $n = 1490$ database: (a) Map of relative abundance in percentages relative to total dinocyst counts and (b) graphs of percentage vs. sea-surface temperature in winter and summer, sea-surface salinity in winter and summer, sea-ice cover, productivity, bathymetry and distance to the coast. In the map, the isobath corresponds to 200 meters of water depth. Source: figures drafted by the authors using MapInfo.

distribution overlapping with that of the other taxa, but that *Spiniferites elongatus* has a distribution distinct from that of *Spiniferites mirabilis-hyperacanthus*, *Spiniferites bentorii* and *Spiniferites delicatus*. It also shows that, when considering relatively high percentages, *Spiniferites bentorii* and *Spiniferites mirabilis-hyperacanthus* share very similar hydrographic domains, but that *Spiniferites delicatus* stands out as a high temperature, relatively low salinity taxon. A marked temperature gradient separates this taxon from the low SST pole where *Spiniferites elongatus* largely dominates.

The distribution of *Spiniferites* taxa in the Northern Hemisphere can be further described from multivariate analyses. The results of the CCA on the occurrence of the 67 taxa in relation to 13 environmental parameters at the 1490 sites of the database (Figure 9; Table 4) clearly show that the dinocyst assemblages closely relate to hydrographical conditions. The first axis explains about 42% of the covariance of the species-environments relationship. It primarily correlates with temperature and sea-ice parameters. The second axis explains about 25.4% of the covariance and correlates best with salinity parameters. The third and fourth axes explain about 12.8% and 7.9% of the covariance and are mostly related to productivity and bathymetry and/or distance to the coast, respectively. All *Spiniferites* taxa have positive scores with regard to the first axis and correlate positively with temperature, except *Spiniferites elongatus* that stands out as a low temperature-seasonal sea ice taxon. Similarly, the scores of most *Spiniferites* taxa correlate with salinity, except for *Spiniferites delicatus*, which shows preference for relatively low salinity. Actually, CCA indicates three poles with *Spiniferites elongatus* at the low temperature-low salinity end, *Spiniferites delicatus* at the high temperature-low salinity

Spiniferites lazus
 $n = 52$

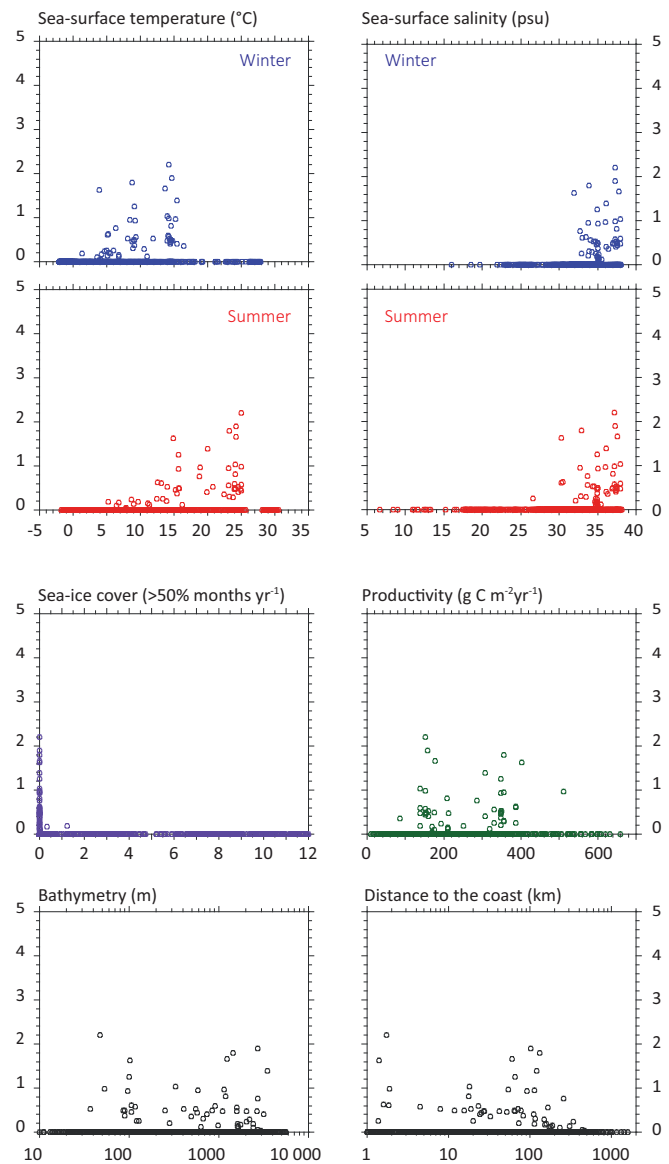


Figure 7. Continued.

end, and a cluster with *Spiniferites mirabilis-hyperacanthus*, *Spiniferites membranaceus*, *Spiniferites bulloideus*, *Spiniferites lazus* and *Spiniferites belerius* aligned towards the high temperature-high salinity end, and *Spiniferites bentorii* at the extremity of this cluster. By contrast, the central position of *Spiniferites ramosus* in the ordination diagram would indicate no clear affinity of the taxon with any of the selected environmental parameters.

The multivariate analyses performed with *Spiniferites* taxa only (Figure 10; Table 5) show similar results, although the relationship was established from redundancy analysis (RDA). The first axis explains about 32% of the species variance and 71.1% of the species-environment covariance. It primarily correlates with temperature and sea-ice parameters. The second axis explains about 12.8% of the covariance and correlates best with salinity parameters. The third axis, explaining about 10.5% of the covariance, mostly relates to

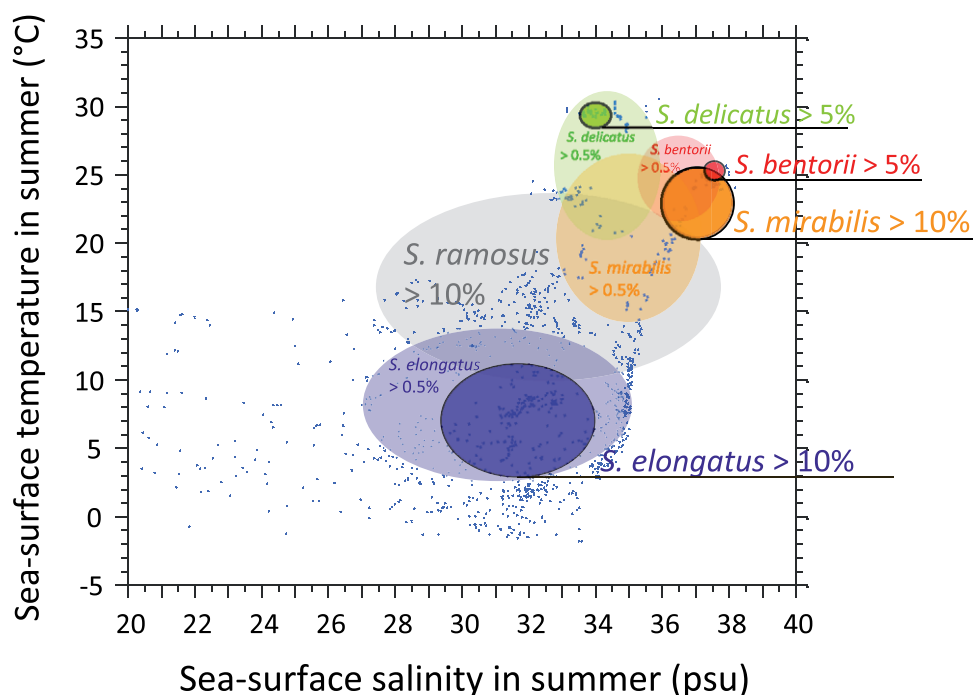


Figure 8. Schematic illustration of the hydrographical domain for the main *Spiniferites* taxa. The ellipses correspond to the average \pm one standard deviation of the summer temperature and salinity at sites where *Spiniferites bentorii*, *Spiniferites delicatus*, *Spiniferites elongatus* and *Spiniferites mirabilis-hyperacanthus* occur ($>0.5\%$) and are common-dominant ($>10\%$ for all, except *Spiniferites bentorii* $>5\%$). The central transparent ellipse corresponds to the average \pm one standard deviation of the summer temperature and salinity at sites where *Spiniferites ramosus* is common or dominant ($>10\%$). Numerical results for averaged environmental parameters corresponding to occurrences of the *Spiniferites* taxa are presented in table 3.

productivity and bathymetry and/or distance to the coast. The ordination diagram also shows three extremes. One extreme is defined by *Spiniferites elongatus* in the low temperature/seasonal sea-ice domain. A second extreme is defined by *Spiniferites delicatus* in the low salinity-high temperature domain. The third extreme is defined by *Spiniferites mirabilis-hyperacanthus* and *Spiniferites bentorii* in the high temperature and high salinity domain. All other taxa have a relatively central position.

4. Discussion

4.1. The spiniferites taxa: their diversity and occurrences

Spiniferites is one of the most common genera of modern dinocyst assemblages, but it includes many species that are difficult to distinguish from each other in palynological slides. Nevertheless, there are taxa that cannot be misidentified based on the concepts used here. These taxa include *Spiniferites ramosus*, *Spiniferites elongatus*, *Spiniferites mirabilis-hyperacanthus*, *Spiniferites bentorii* and *Spiniferites delicatus*, which are distinct from each other in terms of the shape of their body and/or the distribution-shape of their processes and sutures (Table 2; Plates 1–3). They also include *Spiniferites lazus* (Plate 2), which is easy to identify when the base of the processes is clearly visible.

The identity of the other *Spiniferites* taxa in the Northern Hemisphere database (Rochon et al. 1999; de Vernal et al. 2013) is less straightforward. They are usually not very abundant (Table 1) and lack unequivocal criteria of identification: the close similarity of *Spiniferites bulloideus* to *Spiniferites*

ramosus explains why both taxa are often grouped together; *Spiniferites belerius* with more or less expanded septa, mostly in the antapical area is not always easy to identify. In case of doubt in the identification to species level, specimens of *Spiniferites belerius* may have been counted as *Spiniferites* spp. or grouped with *Spiniferites membranaceus* during routine analyses. In addition, the informal taxon *Spiniferites* spp. granular, which was introduced to identify granulate thick-walled specimens (mostly) from the Mediterranean Sea (Mangin 2002) and the northwest North Pacific (Bonnet et al. 2012), may include several species and would require further observations for standardization of consensual operational taxonomy.

Other *Spiniferites* species have been described from recent or modern sediments of the Northern Hemisphere. They notably include *Spiniferites cruciformis* Wall & Dale in Wall et al. 1973, reported to occur in the Caspian Sea, Black Sea and eastern Mediterranean Sea (cf. Zonneveld et al. 2013), but has also been assigned questionably to freshwater or brackish-water environments (Kouli et al. 2001). They also include *Spiniferites hainanensis* Sun & Song 1992 described from sediments along the Chinese coast and reported by Limoges et al. (2018) to occur in other warm environments such as the Marmara Sea and Gulf of California. The cyst of *Gonyaulax baltica* Ellegaard et al. 2002 reported from the Baltic Sea and showing similarities with *Spiniferites bulloideus* is possibly another distinct species (Ellegaard et al. 2002). A few species described from upper Quaternary sediments and possibly extending towards modern can also be mentioned. One of them is *Spiniferites alaskensis* Marret et al. 2001b ex Marret in Fensome & Williams 2004, described from last

interglacial sediments of the northeast Pacific Ocean (Marret et al. 2001b). The cysts referred to as *Achomosphaera andalousiensis* Jan du Chêne 1977, which are very recognizable by their fenestrate processes tips (Head 1993, 1997; Penaud et al. 2008), represent another one. *Achomosphaera andalousiensis* occurs occasionally in recent sediments of the western Mediterranean Sea but seems to be more important in the Miocene, Pliocene and Pleistocene (e.g. de Vernal et al. 1992b). The number of modern *Spiniferites* species might well be higher than what reported in the database. Because the species diversity is usually higher under warm climate (cf. de Vernal & Marret 2007), special care in the taxonomy of *Spiniferites* taxa will be critical when extending the reference database towards low latitudes (cf. for ex., Limoges et al. 2013). In this context, the newly described taxon *Spiniferites multisphaerus* Price & Pospelova 2014 reported from the Gulf of California (cf. Price & Pospelova 2014) has to be mentioned here. There are a few other *Spiniferites* species that were reported from Quaternary deposits (see Mertens et al. 2018), but there are not discussed here because of their very low occurrences.

4.2. The usefulness of *spiniferites* taxa in palaeoceanography

In its present state, the standardized database of the Northern Hemisphere (de Vernal et al. 2013) includes seven taxonomic entities of *Spiniferites* that are distinct from each other, some of them occurring in high number in many surface sediment samples: *Spiniferites bentorii*, *Spiniferites delicatus*, *Spiniferites elongatus*, *Spiniferites mirabilis-hyperacanthus*, *Spiniferites ramosus*, *Spiniferites lazus* and *Spiniferites membranaceus*. The question whether or not these taxa are useful for assessing hydrographical conditions is discussed below.

Spiniferites elongatus* vs. *Spiniferites mirabilis-hyperacanthus – The hydrographical conditions under which high numbers of *Spiniferites elongatus* (>10%) and *Spiniferites mirabilis-hyperacanthus* (>10%) occur in the n=1490 database clearly illustrate their respective affinities for two distinct hydrographical domains. Maximum relative abundances of *Spiniferites elongatus* characterize relatively low saline (31.8±2.4 psu) and cool (7.1±3.8°C) marine waters in summer and seasonal sea-ice cover (4.5±3.4 months/y⁻¹ >50%) in winter, whereas *Spiniferites mirabilis-hyperacanthus* is rather associated to mild-warm (14.2±1.1°C in winter and 23.2±2.7°C in summer) highly saline waters (37.0±0.9 psu in both winter and summer). The distribution of these two taxa with occurrence greater than 0.5% does not show any overlap (Figure 8). Therefore, these taxa represent endmembers within a subpolar to warm temperate gradient, respectively. Such pattern is also obvious from Holocene and late Quaternary sedimentary records. *Spiniferites elongatus* is a typical component of Holocene assemblages in subarctic basins such as the Labrador Sea and Baffin Bay (e.g. Gibb et al. 2015), the Greenland Sea (e.g. Solignac et al. 2006; Van Nieuwenhove et al. 2016), the Barents Sea (Voronina et al. 2001), the Laptev Sea (Klyuvitkina & Bauch 2006), the

Table 3. Surface ocean parameters (mean and standard deviation) at sites where the *Spiniferites* taxa occur from occasionally (>5% or >10%), SST and SSS are respectively sea-surface temperature and sea-surface salinity. The data are schematically illustrated in Figure 8.

Occurrence	<i>S. belerius</i>		<i>S. bentorii</i>		<i>S. bulloideus</i>		<i>S. delicatus</i>		<i>S. elongatus</i>		<i>S. lazus</i>		<i>S. membranaceus</i>		<i>S. mirabilis-hyperacanthus</i>		<i>S. ramosus</i>		<i>S. spp. granularis</i>	
	Present (>0.5%)	Common (>5%)	Present (>0.5%)	Common (>5%)	Present (>0.5%)	Common (>5%)	Present (>0.5%)	Common (>5%)	Present (>0.5%)	Common (>10%)	Present (>0.5%)	Common (>10%)	Present (>0.5%)	Common (>10%)	Present (>0.5%)	Common (>10%)	Present (>0.5%)	Common (>10%)	Present (>0.5%)	Common (>10%)
n	62	28	56	28	56	28	104	22	907	60	22	42	289	87	808	66	42	66	42	42
SST - summer (°C)*	22.9±3.1	23.5±2.6	22.1±4.2	25.3±5.4	22.1±4.2	25.3±5.4	25.3±5.4	29.2±0.5	8.9±5.6	7.1±3.8	20.6±4.4	19.9±4.1	20.4±5.8	23.2±2.7	13.9±7.1	17.2±6.4	22.2±4.9	17.2±6.4	22.2±4.9	22.2±4.9
SST - August (°C)	23.7±3.3	24.4±2.8	23.0±4.4	25.7±5.1	23.0±4.4	25.7±5.1	25.7±5.1	29.5±0.5	9.6±5.8	7.7±4.0	21.4±4.6	20.6±4.3	21.0±5.8	24.1±2.8	14.6±7.1	18.0±6.5	23.4±4.7	18.0±6.5	23.4±4.7	23.4±4.7
SSS - summer (psu)*	36.7±1.3	37.1±1.4	35.8±3.1	34.3±1.6	35.8±3.1	34.3±1.6	34.0±0.6	31.1±3.8	31.1±3.8	31.8±2.4	35.1±2.5	35.3±2.6	34.6±2.4	37.0±0.9	32.0±4.0	33.2±5.2	36.6±1.9	33.2±5.2	36.6±1.9	36.6±1.9
SSS - August (psu)	36.7±1.4	37.0±1.5	37.0±0.2	34.3±1.6	37.0±0.2	34.3±1.6	34.0±0.6	30.9±4.0	30.9±4.0	31.4±2.5	35.0±2.5	35.3±2.6	34.6±2.4	37.0±0.9	31.9±4.0	33.2±5.1	36.6±1.9	33.2±5.1	36.6±1.9	36.6±1.9
SST - winter (°C)	13.7±2.6	13.8±2.1	14.3±0.2	18.6±8.0	12.4±4.5	18.6±8.0	18.6±8.0	24.9±3.4	1.9±4.1	0.9±4.3	11.1±3.8	11.7±4.8	12.2±5.9	14.2±1.1	5.9±6.9	8.5±5.5	12.2±5.4	8.5±5.5	12.2±5.4	12.2±5.4
SST - February (°C)	13.5±2.5	13.7±2.0	14.1±0.3	18.4±8.0	12.3±4.4	18.4±8.0	18.4±8.0	24.6±3.5	1.9±4.0	1.0±4.2	10.9±3.7	11.6±4.7	12.1±5.9	14.0±1.1	5.8±6.9	8.3±5.5	12.0±5.6	8.3±5.5	12.0±5.6	12.0±5.6
SSS - winter (psu)	36.8±1.2	37.1±1.4	37.7±0.2	34.6±1.4	36.1±2.4	34.6±1.4	34.3±0.4	32.6±2.2	32.6±2.2	33.7±1.3	35.5±1.9	35.3±2.6	35.0±1.9	37.0±0.9	33.1±2.7	34.1±3.6	36.7±1.8	34.1±3.6	36.7±1.8	36.7±1.8
SSS - February (psu)	36.8±1.2	37.1±1.2	37.7±0.2	34.6±1.4	36.2±2.5	34.6±1.4	34.2±0.2	32.8±2.3	32.8±2.3	33.7±1.3	35.6±1.9	35.7±2.0	35.0±1.9	37.0±0.9	33.1±2.8	34.2±3.6	36.7±1.8	34.2±3.6	36.7±1.8	36.7±1.8
Productivity (gC/m ² y)	199±78	173±65	144±11	211±97	298±115	302±97	302±97	227±116	227±116	159±75	279±112	268±96	272±109	191±70	277±128	267±121	169±39	277±128	267±121	169±39
Sea-ice cover (months/y ⁻¹)	0	0	0.2±1.2	0±0.2	0.2±1.2	0±0.2	0	3.2±3.6	3.2±3.6	4.5±3.4	0	0	0±0.1	0	1.3±2.4	0.6±1.4	0.3±0.6	1.3±2.4	0.6±1.4	0.3±0.6
Sea-ice concentration (/10)	0	0	0.2±1.0	0±0.2	0.2±1.0	0±0.2	0	2.6±2.9	2.6±2.9	3.6±2.7	0	0	0±0.1	0	1.1±1.9	0.5±1.2	0.2±0.4	1.1±1.9	0.5±1.2	0.2±0.4
Bathymetry (m)	1299±1133	1250±914	1227±680	691±1015	1049±1092	1202±1520	859±1300	1077±1285	817±1017	1202±1520	859±1300	1077±1285	1415±1305	1468±1177	819±1041	530±743	992±802	1415±1305	1468±1177	992±802
Distance to the coast (km)	70±117	53±46	63±108	52±67	63±108	52±67	50±33	126±128	126±128	193±205	60±67	66±60	139±202	93±180	95±108	50±62	80±205	139±202	93±180	80±205

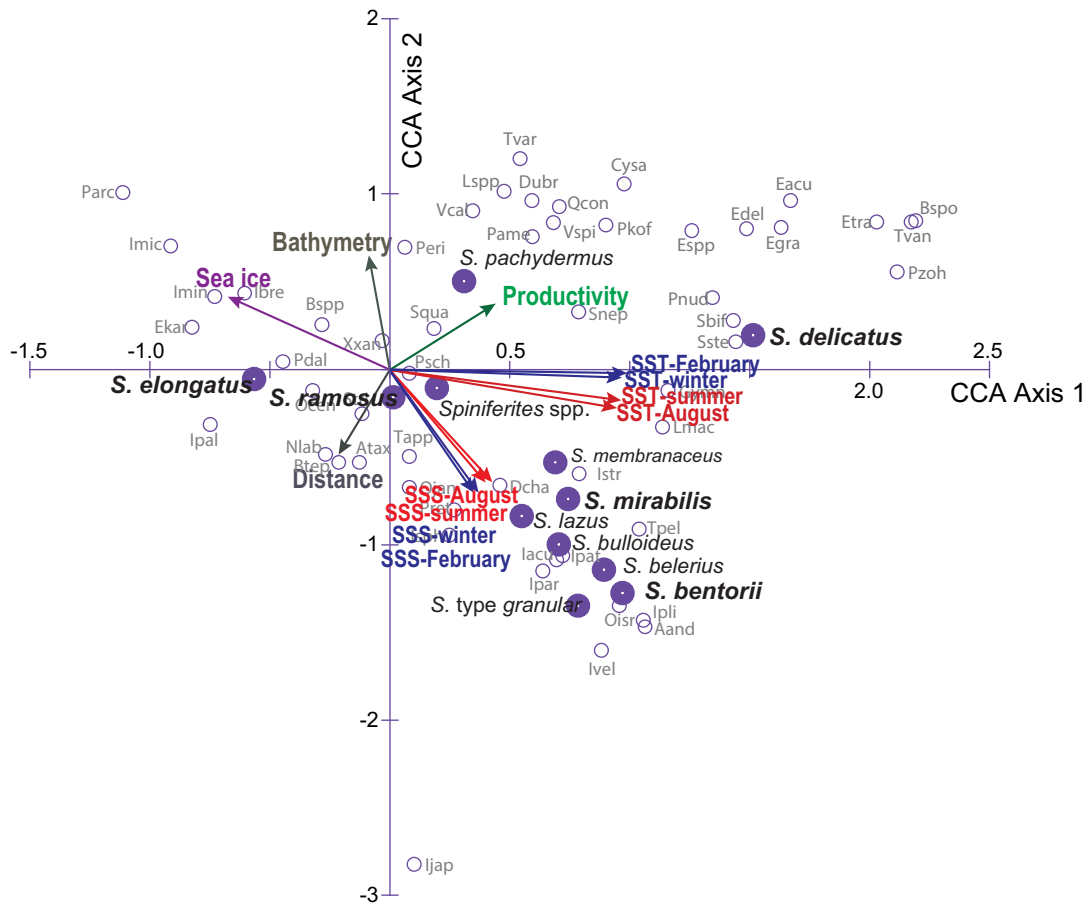


Figure 9. Ordination diagram of the results of canonical correspondence analyses (CCA) on the taxa distribution and sea-surface conditions in the database that includes 67 taxa and 13 environmental parameters at 1490 sites (cf. Table 4 for numerical results).

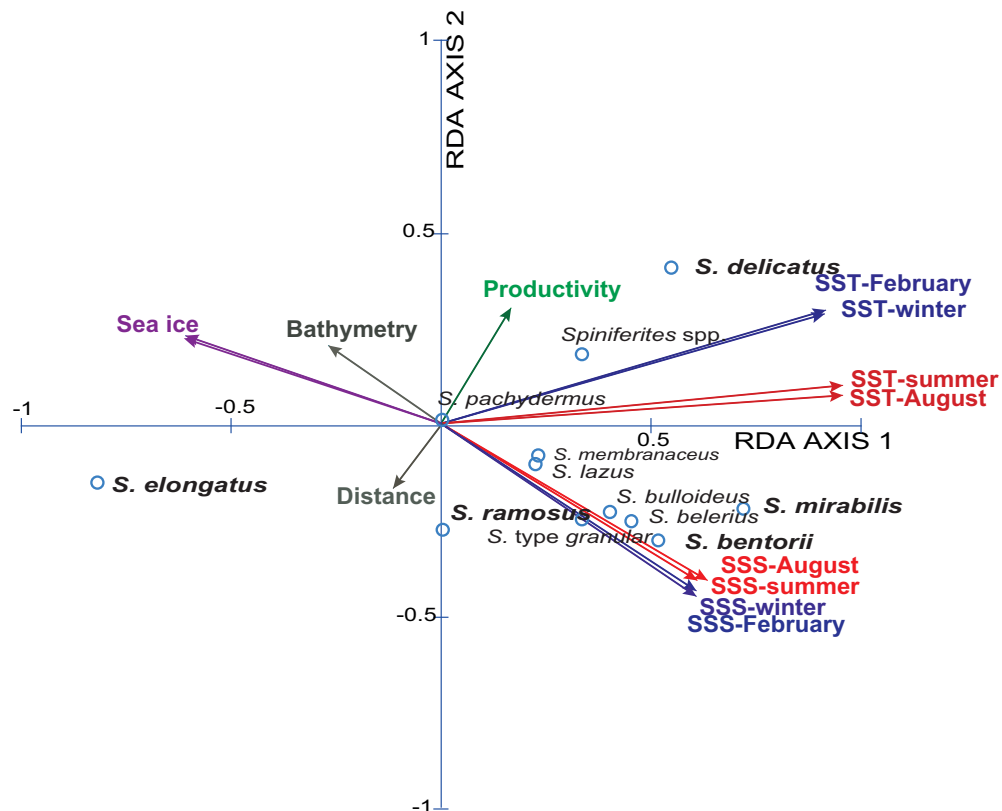


Figure 10. Ordination diagram of the results of redundancy analyses (RDA) on the taxa distribution and sea-surface conditions in the database that includes 12 *Spiniferites* taxa and 13 environmental parameters at 697 sites (cf. Table 5 for numerical results).

Table 4. Results of canonical correspondence analysis (CCA) on the taxa distribution and sea-surface conditions in the database that includes 67 taxa and 13 environmental parameters at 1490 sites (cf. Figure 9 for the ordination diagram). SST and SSS are respectively sea-surface temperature and sea-surface salinity.

Canonical Correspondence Analysis (CCA) - 1490 sites
 67 taxa (log transformed)
 13 environmental parameters

	Axis 1	Axis 2	Axis 3	Axis 4
Eigenvalues	.4339	.2629	.1327	.0819
Spiniferites taxa scores				
<i>S. belerius</i>	.8961	-1.1475	.5918	-.6370
<i>S. bentorii</i>	.9767	-1.2800	.7971	-.8380
<i>S. bulloideus</i>	.7076	-1.0036	.4151	-.5974
<i>S. delicatus</i>	1.5206	.1895	.4802	-.0509
<i>S. elongatus</i> s.l.	-.5614	-.0608	-.0077	-.0831
<i>S. lazus</i>	.6261	-.7548	.0709	-.6222
<i>S. membranaceus</i>	.6957	-.5362	-.0332	-.4142
<i>S. mirabilis-hyperacanthus</i>	.7488	-.7462	.1552	-.0976
<i>S. ramosus</i>	.0193	-.1640	-.1977	-.3374
<i>S. pachydermus</i>	.3160	.4973	-.8615	-.8468
<i>Spiniferites</i> spp.	.2007	-.1122	-.1234	-.1473
<i>Spiniferites</i> spp. granular	.7896	-1.3540	.7841	-.8788
Correlation of environmental variables with axes				
SST-February	.9454	-.0064	.0534	.0859
SSS-February	.3051	-.5248	.1701	-.0712
SST-winter	.9480	-.0077	.0468	.0852
SSS-winter	.3222	-.5280	.1576	-.0683
SST-August	.8833	-.1660	-.0147	-.1095
SSS-August	.3791	-.4774	.0453	-.0317
SST-summer	.8990	-.1419	-.0174	-.0951
SSS-summer	.3519	-.4812	.0828	-.0131
Sea-ice cover (months/y-1)	-.6133	.2865	.4994	.0601
Sea-ice concentration	-.6163	.2865	.5005	.0626
Productivity	.3902	.2662	-.5635	-.0560
Distance to the coast	-.1770	-.3655	-.0885	.5698
Bathymetry	-.0752	.4687	.0933	-.5378

Table 5. Results of redundancy analysis (RDA) on the taxa distribution and sea-surface conditions in the database that includes 12 *Spiniferites* taxa and 13 environmental parameters at 697 sites (cf. Figure 10 for the ordination diagram).

Redundancy Analysis (RDA) - 697 sites
 12 taxa (log transformed)
 13 environmental parameters

	Axis 1	Axis 2	Axis 3
Eigenvalues	.3230	.0584	.0484
Spiniferites taxa scores			
<i>S. belerius</i>	.4564	-.2562	.1001
<i>S. bentorii</i>	.5195	-.3064	.0963
<i>S. bulloideus</i>	.4037	-.2327	.0461
<i>S. delicatus</i>	.5500	.4049	.0364
<i>S. elongatus</i>	-.8171	-.1563	.0361
<i>S. lazus</i>	.2268	-.1072	-.0195
<i>S. membranaceus</i>	.2338	-.0845	-.0176
<i>S. mirabilis-hyperacanthus</i>	.7231	-.2249	.1023
<i>S. ramosus</i>	.0054	-.2792	-.4406
<i>S. pachydermus</i>	.0043	.0081	-.0150
<i>Spiniferites</i> spp.	.3374	.1782	-.3555
<i>Spiniferites</i> spp. granular	.3382	-.2527	.0861
Correlation of environmental variables with axes			
SST-February	.8099	.1896	.0503
SSS-February	.5238	-.2789	.3143
SST-winter	.8123	.1912	.0473
SSS-winter	.5288	-.2851	.3273
SST-August	.8342	.0523	-.1229
SSS-August	.5463	-.2599	.2016
SST-summer	.8415	.0706	-.1128
SSS-summer	.5354	-.2612	.2362
Sea-ice cover (months/y ⁻¹)	-.5385	.1444	.2640
Sea-ice concentration	-.5408	.1409	.2657
Productivity	.1486	.1884	-.4079
Distance to the coast	-.1021	-.1023	.2883
Bathymetry	-.2387	.1300	-.1779

Chukchi Sea (de Vernal et al. 2005b; McKay et al. 2008), the Bering Sea (Radi et al. 2001) and the Gulf of Alaska (de Vernal & Pedersen 1997; Marret et al. 2001b). In contrast, *Spiniferites mirabilis-hyperacanthus*, which is absent from the above mentioned subarctic environment, is common in Holocene sediments of warm environments such as the Mediterranean Sea (e.g. Rouis-Zargouni et al. 2010), the Bay of Biscay (e.g. Zumaque et al. 2017), and the Gulf of Mexico (Limoges et al. 2014). Moreover, *Spiniferites mirabilis* recorded a maximum occurrence peak during the last interglacial or marine isotope stage (MIS) 5e (ca. 128–117 ka), both in the North Atlantic (Eynaud et al. 2004; Penaud et al. 2008; Van Nieuwenhove et al. 2011; Harland et al. 2016) and in the South Pacific (Marret et al. 2001a). The maximum occurrence peak of *Spiniferites mirabilis* during the last interglacial is compatible with the particularly warm conditions that characterized the last interglacial worldwide (e.g. PIGS 2016).

Spiniferites elongatus is a useful taxon despite variations in its morphology concerning the length vs. width ratio of the cyst body and the expansion of the apical and antapical septa. Specimens characterized by a particularly elongate shape and well developed apical-antapical septa, originally assigned to *Spiniferites frigidus*, were reported to be abundant in Baffin Bay, Barents Sea, Bering Sea and Beaufort Sea (e.g. Harland et al. 1980; Harland 1982; Mudie & Short 1985; Radi et al. 2001). Hence, it is tempting to associate the most elongated morphotypes to cold settings. However, systematic observations and measurements of the length and width of the cyst and septa have still not provided a statistically clear relationship between morphometry and environmental parameters (Van Nieuwenhove et al. 2018).

The case of *Spiniferites ramosus* – In contrary to *Spiniferites elongatus* and *Spiniferites mirabilis-hyperacanthus*, *Spiniferites ramosus* is not a taxon with distinctive and thus easy to identify ecological affinities as it can be found in a wide range of environmental settings. It occurs in high proportions (>10%) in cool to warm waters ($8.5 \pm 5.5^\circ\text{C}$ in winter and $17.2 \pm 6.4^\circ\text{C}$ in summer) and at very variable salinity (33.2 ± 5.2 psu). It encompasses areas occupied by *Spiniferites elongatus* and *Spiniferites mirabilis-hyperacanthus* and often occurs as the most common *Spiniferites* taxon at mid latitudes (cf. this study) as well as low latitudes (e.g. Limoges et al. 2013; Hessler et al. 2013). As concluded by Marret & Zonneveld (2003) and Zonneveld et al. (2013) from global data compilations, *Spiniferites ramosus* seems to be very cosmopolitan. However, *Spiniferites ramosus* records a large morphological variability, possibly including more than one species or genotype. What is identified as *Spiniferites ramosus* can relate to co-existing cryptic species. The variable morphology could also reflect a true morphological plasticity of the species that might be a response to environmental stress. In any case, the cosmopolitan distribution of *Spiniferites ramosus* possibly results from the clustering of different species or subspecies that are difficult to distinguish on a routine basis. It is also of note that *Spiniferites ramosus* is a long ranging taxon (lowermost Cretaceous to modern) and that more than 30 infra-specific taxa of *Spiniferites ramosus* have been described (Williams et al. 2017). It can thus be concluded

that the current morphological concept of *Spiniferites ramosus* constitutes an entity with poorly constrained taxonomy, ecological affinity and biostratigraphy.

***Spiniferites bentorii* and *Spiniferites delicatus* as thermophilic species** – In the warmer part of the database, the distribution of *Spiniferites bentorii* and *Spiniferites delicatus* shows distinct characteristics with regard to hydrographic conditions (Figure 8, Table 3). Moreover, both taxa seem to have a neritic distribution as their occurrence is exclusive to sites located relatively close to the coast (<120 km; see Figures 4b and 5b). Relatively high percentages of *Spiniferites delicatus* (>5%) characterize year-round warm environments ($22.9 \pm 0.5^\circ\text{C}$ in winter and $24.9 \pm 3.4^\circ\text{C}$ in summer), rather low salinity around 34 ± 0.6 psu and high productivity (302 ± 97 gC m⁻²y⁻¹). *Spiniferites delicatus*, however, is still represented by a limited number of data points in the Northern Hemisphere reference database (de Vernal et al. 2013), but its known global distribution tends to support affinities for tropical waters (cf. Zonneveld et al. 2013). For example, the ecological affinities identified here from the mid latitudes of the Northern Hemisphere are consistent with the distribution pattern of *Spiniferites delicatus* in the Gulf of Guinea, equatorial Atlantic, where maximum occurrences (up to 80%) are also recorded under temperature and salinity ranging $23\text{--}29^\circ\text{C}$ and 34–35 psu (Marret 1994; Marret & Zonneveld 2003).

The environments with relatively high occurrence of *Spiniferites bentorii* (>5%) are different from those recording high percentages of *Spiniferites delicatus* (>5%). In the mid latitude of the Northern Hemisphere, *Spiniferites bentorii* seems to characterize areas with important contrast of seasonal temperature gradients ($14.3 \pm 0.2^\circ\text{C}$ in winter and $24.3 \pm 0.4^\circ\text{C}$ in summer), high salinity (37.6 ± 0.3 psu) and lower productivity (144 ± 11 gC m⁻²y⁻¹). However, *Spiniferites delicatus* is also present in the Black Sea (up to 10%), where salinity can be very low, thus suggesting tolerance for lower salinity (e.g. Mudie et al. 2007). The species has also been reported (up to 6%) from North American temperate, nutrient-rich estuarine systems with an average SSS of ~ 27 psu (Pospelova et al. 2002; Price & Pospelova 2011). From its worldwide distribution compiled by Zonneveld et al. (2013), *Spiniferites bentorii* tends to display affinities for warm conditions with large seasonal temperature contrasts, and with tolerance for wide salinity ranges.

Spiniferites membranaceus* and *Spiniferites lazus – *Spiniferites membranaceus* and *Spiniferites lazus* are distinct entities, but they are not often abundant. In the mid-high latitudes of the Northern Hemisphere, they share similar warm temperate domains. However, their preferred environments might be at lower latitudes and for warmer conditions (cf. Zonneveld et al. 2013). For example, *Spiniferites membranaceus* is common in intertropical areas of the Indian Ocean (e.g. Hessler et al. 2013) and the South China Sea (Kawamura 2004). The known distribution of *Spiniferites lazus* in time and space is limited, with documented occurrence mostly restricted to late Quaternary sediment of British Isles (Reid 1974; Marret & Scourse 2002) and Mediterranean Sea (Turon & Londeix 1988; Mangin 2002). *Spiniferites lazus*, however,

recorded peaks of abundance during cold episodes of the last glacial stage in the subtropics (Marret & Turon 1994; Penaud et al. 2010) and is quite abundant (more than 20%) in the sediments of the Holocene thermal optimum of the Celtic Sea (Marret et al. 2004).

5. Conclusions

Despite a wide range of morphological variations, taxonomic uncertainties and the possibility of cryptic species, some of the main species of *Spiniferites* routinely identified and counted for population analyses are very useful tracers of sea-surface conditions. These species principally include *Spiniferites elongatus*, *Spiniferites mirabilis-hyperacanthus*, *Spiniferites bentorii* and *Spiniferites delicatus*, which are diagnostic to identify subpolar, cool temperate, warm temperate and tropical conditions. In particular, the occurrence of *Spiniferites elongatus* and *Spiniferites mirabilis-hyperacanthus*, which are common in marine sediments, is very useful to distinguish subpolar from warm temperate environments. *Spiniferites bentorii* and *Spiniferites delicatus* are also diagnostic to document warm conditions although their occurrence is not as common. Other species might well be useful at mid-low latitudes but some effort to develop an operational taxonomy to ascertain consistent identification of taxa is needed.

One particularity of the dinocyst database as compared to other palaeoceanographical tracers such as planktic foraminifers or coccoliths is the possibility to include both nearshore and offshore, shallow and deep sites. This results in large ranges of SSSs and in various combinations of SST and SSS and winter vs. summer extremes. Shelf environments are indeed often prone to stratification of the upper water masses, which leads to low thermal inertia and therefore large temperature changes from winter to summer in high latitudes. Hence, among *Spiniferites* taxa, some show more affinities for nearshore environments characterized by low salinity. This seems to be the case for *Spiniferites delicatus*. The large morphological plasticity displayed by other taxa such as *Spiniferites ramosus*, might actually be an illustration of the adaptation to various and variable conditions. Attentive examination of their morphological ranges can be relevant as they might well reflect different environmental conditions.

Acknowledgements

We are grateful to the anonymous reviewer of the journal and to Karin Zonneveld who made a thorough examination of the original manuscript and provided useful comments. This study is a contribution supported by research funds from the Natural Sciences and Engineering Council (NSERC) of Canada and the Fonds de recherche du Québec - Nature et technologies (FRQNT).

Disclosure statement

No potential conflict of interest was reported by the author.

References

- Behrenfeld MJ, Falkowski PG. 1997. Photosynthetic rates derived from satellite-based chlorophyll concentration. *Limnol Oceanogr.* 42(1): 1–20.
- Bonnet S, de Vernal A, Gersonde R, Lembke-Jene L. 2012. Modern distribution of dinocysts from the North Pacific Ocean (37–64 °N, 144 °E–148 °W) in relation to hydrographic conditions, sea-ice and productivity. *Mar Micropaleontol.* 84–85:87–113.
- Bujak JP. 1984. Cenozoic dinoflagellate cysts and acritarchs from the Bering Sea and northern North Pacific, DSDP Leg 19. *Micropaleontology.* 30:80–212.
- Conkright ME, Locarnini RA, Garcia HE, O'Brien TD, Boyer TP, Stephens C, Antonov JI. 2002. World Ocean Atlas 2001: Objective analyses, data statistics, and figures: CD-ROM documentation. US Department of Commerce, National Oceanic and Atmospheric Administration, National Oceanographic Data Center, Ocean Climate Laboratory.
- de Vernal A, Marret F. 2007. Organic-walled dinoflagellates: tracers of sea-surface conditions. In: Hillaire-Marcel C, de Vernal A eds. *Proxies in Late Cenozoic Paleoceanography*. Elsevier; p. 371–408.
- de Vernal A, Mudie PJ. 1989. Pliocene to Recent Palynostratigraphy at ODP Sites 646 and 647, eastern and southern Labrador Sea. Arthur M, Srivastava S, Clement B eds. *Proceedings of the Ocean Drilling Program 105B*. Texas A & M University; p. 401–422.
- de Vernal A, Pedersen T. 1997. Micropaleontology and palynology of core PAR 87 A-10: a 30,000 years record of paleoenvironmental changes in the Gulf of Alaska, northeast North Pacific. *Paleoceanography.* 12(6):821–830.
- de Vernal A, Bilodeau G, Hillaire-Marcel C, Kassou N. 1992. Quantitative assessment of carbonate dissolution in marine sediments from foraminifer linings vs. shell ratios: example from Davis Strait, NW North Atlantic. *Geol.* 20(6):527–530.
- de Vernal A, Londeix L, Harland R, Morzadec-Kerfourn M-T, Mudie PJ, Turon J-L, Wrenn J. 1992b. The Quaternary organic walled dinoflagellate cyst of the North Atlantic Ocean and adjacent seas: ecostratigraphic and biostratigraphic records. In: Head MJ, Wrenn JH eds. *Neogene and Quaternary dinoflagellate cysts and acritarchs*. Dallas: AASP Foundation; p. 289–328.
- de Vernal A, Rochon A, Hillaire-Marcel C, Turon J-L, Guiot J. 1993. Quantitative reconstruction of sea-surface conditions, seasonal extent of sea-ice cover and meltwater discharges in high latitude marine environments from dinoflagellate cyst assemblages. *Proceedings of the NATO Workshop on Ice in the Climate system*. NATO ASI Series. 112:611–621.
- de Vernal A, Rochon A, Turon J-L, Matthiessen J. 1997. Organic-walled dinoflagellate cysts: palynological tracers of sea-surface conditions in middle to high latitude marine environments. *Geobios.* 30(7):905–920.
- de Vernal A, Henry M, Matthiessen J, Mudie PJ, Rochon A, Boessenkool K, Eynaud F, Grøsfjeld K, Guiot J, Hamel D, et al. 2001. Dinoflagellate cyst assemblages as tracers of sea-surface conditions in the northern North Atlantic, Arctic and sub-Arctic seas: the new “n = 677” database and application for quantitative palaeoceanographical reconstruction. *J Quaternary Sci.* 16(7):681–699.
- de Vernal A, Eynaud F, Henry M, Hillaire-Marcel C, Londeix L, Mangin S, Matthiessen J, Marret F, Radi T, Rochon A, et al. 2005. Reconstruction of sea-surface conditions at middle to high latitudes of the Northern Hemisphere during the Last Glacial Maximum (LGM) based on dinoflagellate cyst assemblages. *Quat Sci Rev.* 24(7–9):897–924.
- de Vernal A, Hillaire-Marcel C, Darby D. 2005b. Variability of sea ice cover in the Chukchi Sea (western Arctic Ocean) during the Holocene. *Paleoceanography.* 20:PA4018.
- de Vernal A, Rochon A, Fréchette B, Henry M, Radi T, Solignac S. 2013. Reconstructing past sea ice cover of the Northern hemisphere from dinocyst assemblages: status of the approach. *Quat Sci Rev.* 79: 122–134.
- Ellegaard M, Lewis J, Harding I. 2002. Cyst-theca relationship, life cycle, and effects of temperature and salinity on the cyst morphology of *Gonyaulax baltica* sp. nov. (Dinophyceae) from the Baltic Sea area. *J Phycol.* 38(4):775–789.

- Eyraud F, Turon J-L, Duprat J. 2004. Comparison of the Holocene and Eemian palaeoenvironments in the South Icelandic Basin: dinoflagellate cysts as proxies for the North Atlantic surface circulation. *Rev Palaeobot Palynol.* 128(1-2):55-79.
- Gibb OT, Steinhauer S, Fréchette B, de Vernal A, Hillaire-Marcel C. 2015. Diachronous evolution of sea surface conditions in the Labrador Sea and Baffin Bay since the last deglaciation. *The Holocene.* 25(12):1882-1897.
- Guiot J, de Vernal A. 2007. Transfer functions: methods for quantitative paleoceanography based on microfossils. In: Hillaire-Marcel C, de Vernal A eds. *Proxies in Late Cenozoic Paleocyanography.* Elsevier; p. 523-563.
- Harland R. 1977. Recent and late Quaternary (Flandrian and Devensian) dinoflagellate cysts from marine continental shelf sediments around the British Isles. *Palaeontographica. Abteilung B.* 164:87-126.
- Harland R. 1982. Recent dinoflagellate cyst assemblages from the southern Barents Sea. *Palynology.* 6(1):9-18.
- Harland R, Reid PC, Dobell P, Norris G. 1980. Recent and sub-recent dinoflagellate cysts from the Beaufort Sea, Canadian Arctic. *Grana.* 19(3):211-225.
- Harland R, Asteman IP, Morley A, Morris A, Harris A, Howe JA. 2016. Latest Quaternary palaeoceanographic change in the eastern North Atlantic based upon a dinoflagellate cyst event ecostratigraphy. *Heliyon.* 2(5):e00114.
- Head MJ. 1993. Dinoflagellates, Sporomorphs, and Other Palynomorphs from the Upper Pliocene St. Erth Beds of Cornwall, Southwestern England. *Mem Paleontol Soc.* 31:1-62.
- Head MJ. 1996. Modern dinoflagellate cysts and their biological affinities. In: Jansonius J & McGregor DC eds. *Palynology: principles and applications.* Dallas: AASP Foundation; p. 1197-1248.
- Head MJ. 1997. Thermophilic dinoflagellate assemblages from the Mid Pliocene of eastern England. *J Paleontol.* 71(02):165-193.
- Heikkilä M, Pospelova V, Hochheim KP, Kuzyk ZZA, Stern GA, Barber DG, Macdonald RW. 2014. Surface sediment dinoflagellate cysts from the Hudson Bay system and their relation to freshwater and nutrient cycling. *Mar Micropaleontol.* 106:79-109.
- Hessler I, Young M, Holzwarth U, Mohtadi M, Lückge A, Behling H. 2013. Imprint of eastern Indian Ocean surface oceanography on modern organic-walled dinoflagellate cyst assemblages. *Marine Micropaleontol.* 101:89-105.
1995. Jongman RHG, ter Braak CJF, Van Tongeren OFR. (Eds.). *Data analysis in community and landscape ecology.* Cambridge: Cambridge University Press.
- Kawamura H. 2004. Dinoflagellate cyst distribution along a shelf to slope transect of an oligotrophic tropical sea (Sunda Shelf, South China Sea). *Phycological Res.* 52(4):355-375.
- Klyuvitkina TS, Bauch HA. 2006. Hydrological changes in the Laptev Sea during the Holocene inferred from the studies of aquatic palynomorphs. *Okeanologiya.* 46:911-921.
- Kouli K, Brinkhuis H, Dale B. 2001. *Spiniferites cruciformis*: a fresh water dinoflagellate cyst? *Rev Palaeobot Palynol.* 113(4):273-286.
- Lewis J, Rochon A, Harding I. 1999. Preliminary observations of cyst-theca relationships in *Spiniferites ramosus* and *Spiniferites membranaceus* (Dinophyceae). *Sgra.* 38(2):113-124.
- Limoges A, Kieft J-F, Radi T, Ruiz-Fernandez AC, de Vernal A. 2010. Dinoflagellate cyst distribution in surface sediments along the southwestern Mexican coast (14.76 ° N to 24.75 ° N). *Mar Micropal.* 76(3-4):104-123.
- Limoges A, Londeix L, de Vernal A. 2013. Organic-walled dinoflagellate cyst distribution in the Gulf of Mexico. *Mar Micropal.* 102:51-68.
- Limoges A, de Vernal A, Van Nieuwenhove N. 2014. Long-term hydrological changes in the northeastern Gulf of Mexico (ODP-625B) during the Holocene and late Pleistocene inferred from organic-walled dinoflagellate cysts. *Palaeogeogr Palaeoclim Palaeoecol.* 414:178-191.
- Limoges A, Londeix L, Mertens KN, Rochon A, Pospelova V, del Carmen Cuéllar T, de Vernal A. 2018. Identification key for Pliocene and Quaternary *Spiniferites* taxa bearing intergonal processes based on observations from estuarine and coastal environments. *Palynology.* 42(S1).
- Londeix L, Zonneveld K, Masure E. 2018. Taxonomy and operational identification of Quaternary species of *Spiniferites* and related genera. *Palynology.* 42(S1).
- Mangin S. 2002. Distribution actuelle des kystes de dinoflagellés en Méditerranée occidentale et application aux fonctions de transfert, vol. 1. *Memoir of DEA; University of Bordeaux*
- Marret F. 1994. Distribution of dinoflagellate cysts in recent marine sediments from the east equatorial Atlantic (Gulf of Guinea). *Rev Palaeobot Palynol.* 84(1-2):1-22.
- Marret F, de Vernal A, Benders F, Harland R. 2001a. of late Quaternary sea-surface conditions at DSDP Site 594 in the southwest Pacific Ocean based on dinoflagellate cyst assemblages. *J Quaternary Sci.* 16(7):739-749. *Reconstruction*
- Marret F, de Vernal A, Pedersen TF, McDonald D. 2001b. Middle Pleistocene to Holocene palynostratigraphy of ODP 887 in the Gulf of Alaska, northeastern North Pacific. *Can J Earth Sci.* 38(3):373-386.
- Marret F, Scourse J. 2003. Control of modern dinoflagellate cyst distribution in the Irish and Celtic seas by seasonal stratification dynamics. *Mar Micropaleontol.* 47(1-2):101-116.
- Marret F, Scourse J, Austin W. 2004. Holocene shelf-sea seasonal stratification dynamics: a dinoflagellate cyst record from the Celtic Sea, NW European shelf. *The Holocene.* 14(5):689-696.
- Marret F, Turon J-L. 1994. Paleohydrology and paleoclimatology off Northwest Africa during the last glacial interglacial transition and the Holocene - palynological evidences. *Mar Geol.* 118(1-2):107-117.
- Marret F, Zonneveld KAF. 2003. Atlas of modern organic-walled dinoflagellate cyst distribution. *Rev Palaeobot Palynol.* 125(1-2):1-200.
- McKay JL, de Vernal A, Hillaire-Marcel C, Not C, Polyak L, Darby D. 2008. Holocene fluctuations in Arctic sea-ice cover: Dinocyst-based reconstructions for the eastern Chukchi Sea. *Can J Earth Sci.* 45(11):1377-1397.
- Mertens KN, Van Nieuwenhove N, Gurdebeke N, Aydin PR, Bogus H, Bringué K, Dale M, De Scheppe B, de Vernal S, Ellegaard A, Grothe M, et al. 2018. Summary of round table discussions about *Spiniferites* and *Achomosphaera* occurring in Pliocene to modern sediments. *Palynology.* 42(S1).
- Mudie PJ, Short SK. 1985. *Marine Palynology of Baffin Bay.* In: Andrews JT ed. *Quaternary Studies of Baffin Island, West Greenland and Baffin Bay.* London: Allen & Unwin; p. 263-308.
- Mudie PJ, Marret F, Aksu AE, Hiscott RN, Gillespie H. 2007. Palynological evidence for climatic change, anthropogenic activity and outflow of Black Sea Water during the late Pleistocene and Holocene: centennial-to decadal-scale records from the Black and Marmara Seas. *Quat Int.* 167-168:73-90.
- Penaud A, Eyraud F, Turon J-L, Zaragosi S, Marret F, Bourillet JF. 2008. Interglacial variability (MIS 5 and MIS 7) and dinoflagellate cysts assemblages in the Bay of Biscay (North Atlantic). *Mar Micropaleontol.* 68(1-2):136-155.
- Penaud A, Eyraud F, Turon J-L, Blamart D, Rossignol L, Marret F, Lopez-Martinez C, Grimalt JO, Malaizé B, Charlier K. 2010. Contrasting paleoceanographic conditions off Morocco during Heinrich events (1 and 2) and the Last Glacial Maximum. *Quat Sci Rev.* 29(15-16):1923-1939.
- PIGS (Past Interglacials Working Group of PAGES) 2016. Interglacials of the last 800,000 years. *Rev Geophys.* 54:162-219.
- Pospelova V, Chmura GL, Boothman WS, Latimer JS. 2002. Dinoflagellate cyst records and human disturbance in two neighboring estuaries, New Bedford Harbor and Apponagansett Bay, Massachusetts (USA). *Sci Total Environ.* 298(1-3):81-102.
- Pospelova V, de Vernal A, Pedersen TF. 2008. Distribution of dinoflagellate cysts in surface sediments from the northeastern Pacific Ocean (43-25 ° N) in relation to sea-surface temperature, productivity and coastal upwelling. *Mar Micropaleontol.* 68(1-2):21-48.
- Pospelova V, Zonneveld KAF, Heikkilä M, Bringué M, Price A, Esenkulova S, Matsuoka K. 2018. Seasonal, annual, and inter-annual *Spiniferites* cyst production: a review of sediment trap studies. *Palynology.* 42(S1).
- Price AM, Pospelova V. 2011. High-resolution sediment trap study of organic-walled dinoflagellate cyst production and biogenic silica flux in Saanich Inlet (BC, Canada). *Mar Micropaleontol.* 80(1-2):18-43.

- Price AM, Pospelova V. 2014. *Spiniferites multisphaerus*, a new dinoflagellate cyst from the Late Quaternary of the Guaymas Basin, Gulf of California, Mexico. *Palynology*. 38(1):101–116.
- Radi T, de Vernal A. 2004. Dinocyst distribution in surface sediments from the northeastern Pacific margin (40–60 °N) in relation to hydrographic conditions, productivity and upwelling. *Rev Paleobot Palynol*. 128(1–2):169–193.
- Radi T, de Vernal A. 2008. Dinocysts as proxy of primary productivity in mid-high latitudes of the Northern Hemisphere. *Mar Micropaleontol*. 68(1–2):84–114.
- Radi T, de Vernal A, Peyron O. 2001. Relationships between dinocyst assemblages in surface sediment and hydrographic conditions in the Bering and Chukchi seas. *J Quaternary Sci*. 16(7):667–681.
- Radi T, Pospelova V, de Vernal A, Barrie JV. 2007. Dinoflagellate cysts as indicators of water quality and productivity in British Columbia estuarine environments. *Mar Micropaleontol*. 62(4):269–297.
- Reid PC. 1974. Gonyaulacacean dinoflagellate cysts from the British Isles. *Nova Hedwigia*. 25:579–637.
- Rochon A, de Vernal A, Turon JL, Matthiessen J, Head MJ. 1999. Distribution of Dinoflagellate Cysts in Surface Sediments from the North Atlantic Ocean and Adjacent Basin and Quantitative Reconstruction of Sea-Surface Parameters. *AASP Contrib Ser*. 35:146. pp.
- Rochon A, Lewis J, Ellegaard M, Harding IC. 2009. The Gonyaulax spinifera (Dinophyceae) "complex": Perpetuating the paradox? *Rev Paleobot Palynol*. 155(1–2):52–60.
- Rosignol M. 1964. Hystrichosphères du Quaternaire en Méditerranée orientale, dans les sédiments Pléistocènes et les boues marines actuelles. *Rev Micropaléontol*. 7:83–99.
- Rouis-Zargouni I, Turon J-L, Londeix L, Essallami L, Kallel N, Sicre M-A. 2010. Environmental and climatic changes in the central Mediterranean Sea (Siculo-Tunisian Strait) during the last 30 ka based on dinoflagellate cyst and planktonic foraminifera assemblages. *Palaeogeogr Palaeoclim Palaeoeco*. 285(1–2):17–29.
- Solignac S, Giraudeau J, de Vernal A. 2006. Holocene sea-surface conditions in the western Nordic Seas: spatial and temporal heterogeneities. *Paleoceanography*. 21:PA2004.
- Xuekun S, Zhichen S. 1992. Quaternary dinoflagellates from arenaceous dolomite in Hainan Island. *Acta Micropal Sinica*. 9:45–52.
- Ter Braak CJF, Smilauer P. 2002. Canoco for Windows Version 4.5. Biometris Plant Research International, Wageningen, The Netherlands.
- Turon J-L, Londeix L. 1988. Les assemblages de kystes de dinoflagellés en Méditerranée occidentale (mer d'Alboran). Mise en évidence de l'évolution des paléoenvironnements depuis le dernier maximum glaciaire. *Bulletin Des Centres de Recherches Exploration-Production Elf-Aquitaine*. 12:313–344.
- Vancoppenolle M, Meiners KM, Michel C, Bopp L, Brabant F, Carnat G, Delille B, Lannuzel D, Madec G, Moreau S, et al. 2013. Role of sea ice in global biogeochemical cycles: emerging views and challenges. *Quat Sci Rev*. 79:207–230.
- Van Nieuwenhove N, Bauch HA, Eynaud F, Kandiano E, Cortijo E, Turon J-L. 2011. Evidence for delayed poleward expansion of North Atlantic surface waters during the last interglacial (MIS 5e). *Quat Sci Rev*. 30(7–8):934–946.
- Van Nieuwenhove N, Baumann A, Matthiessen J, Bonnet S, de Vernal A. 2016. Sea surface conditions in the southern Nordic Seas during the Holocene based on dinoflagellate cyst assemblages. *The Holocene*. 26(5):722–735.
- Van Nieuwenhove N, Potvin É, Heikkilä M, Pospelova V, Mertens KN, Masure E, Kucharska M, Yang EJ, Chomérat N, Zajaczkowski M. 2018. Taxonomic revision of *Spiniferites elongatus* (the resting stage of *Gonyaulax elongata*) based on morphological and molecular analyses. *Palynology*. 42(S1).
- Vásquez-Bedoya LF, Radi T, Ruiz-Fernández AC, de Vernal A, Machain-Castillo ML, Kieft J-F, Hillaire-Marcel C. 2008. Centennial record of organic-walled dinoflagellate cysts and benthic foraminifera in coastal sediments from the Gulf of Tehuantepec, eastern equatorial Pacific. *Mar Micropaleontol*. 68(1–2):49–65.
- Voronina E, Polyak L, de Vernal A, Peyron O. 2001. Holocene variations of sea-surface conditions in the southeastern Barents Sea based on palynological data. *J Quaternary Sci*. 16(7):717–727.
- Wall D, Dale B, Harada K. 1973. Descriptions of new fossil dinoflagellates from the Late Quaternary of the Black Sea. *Micropaleontology*. 19(1): 18–31.
- Williams GL, Fensome RA, MacRae RA. 2017. The Lentin and Williams index of fossil dinoflagellates 2017 edition. *AASP Contrib Ser*. 48.
- Wrenn JH. 1988. Differentiating species of the dinoflagellate cyst genus *Nematosphaeropsis* Deflandre & Cookson 1955. *Palynology*. 12(1): 129–150.
- Zonneveld KAF, Marret F, Versteegh GJM, Bonnet S, Bouimetarhan I, Crouch E, de Vernal A, Elshanawany R, Edwards L, Esper O, et al. 2013. Atlas of modern dinoflagellate cyst distribution based on 2405 datapoints. *Rev Paleobot Palynol*. 191:1–197.
- Zonneveld KAF, Pospelova V. 2015. A determination key for modern dinoflagellate cysts. *Palynology*. 39(3):387–407.
- Zumaque J, Eynaud F, de Vernal A. 2017. Holocene paleoceanography of the Bay of Biscay: evidence for West-East linkages in the North Atlantic based on dinocyst data. *Palaeogeogr Palaeoclim Palaeoeco*. 468:403–413.